Lake and reservoir volume variability from satellite imagery data

An assessment of the usability of high-resolution digital elevation models to extract water levels

D.H. van der Heide
Student number: 4715411

TU Delft

Lake and reservoir volume variability from satellite imagery data

An assessment of the usability of high-resolution digital elevation models to extract water levels

D.H. (Daan) van der Heide

in partial fulfilment of the requirements for the degree of

Master of Science
in Civil Engineering

at the Delft University of Technology,
to be defended publicly on Tuesday November 9th, 2021, at 09:00 AM.

Supervisor:	Dr. ir. S.L.M. (Stef) Lhermitte	TU Delft
Thesis committee:	Prof. dr. ir. N.C. (Nick) van de Giesen	TU Delft
	Dr.ir. D.C. (Cornelis) Slobbe	TU Delft
	Dr.ir. G. (Gennadii) Donchyts	Deltares
	A. (Arjen) Haag, MSc	Deltares

Preface

My background before writing this thesis was in hydrographic surveying. Thus, allowing me to use my practical knowledge of using remote sensing instruments in the application presented in this master thesis. The thesis is written in completion of my master in remote sensing.

First of all, I want to thank my supervisors at Deltares, Gennadii Donchyts and Arjen Haag, for guiding me in the field of remote sensing and sharing your knowledge on lakes and reservoirs.

Secondly, I want to thank my day-to-day supervisors, Stef Lhermitte and Cornelis Slobbe, from the TU Delft for keeping my focus on the aim of my thesis, their knowledge of the subject, and always taking the time for me to explain the things that I did not see at first. And Nick van de Giesen, I want to thank you for supplying the papers that became the backbone of my research.

Also, I like to thank my friends, who pre-read my thesis, which made it now readable for you, my parents and my brothers, who supported me on this fantastic 8-years journey to my graduation.

Likewise, I want to thank my housemates Niek and Kasper, who always listened to me during the debug hours, my stories and opinions about the subject, and then kept me on track with a nice cup of ice coffee.

D.H. van der Heide
Delft, November 2021

Abstract

Recent research suggested that the digital elevation models can be considered, as an alternative to the altimetry data. However, the water prohibits the ability of monitoring the construction the waterbed, due to the loss of the returning signal. The elevation models have therefore a flat surface, which prohibits the extraction of the water level and volume variability.

The goal of this thesis was to develop a tool, that uses the elevations where no flatting had occurred, and create a linear representation of the shape of the lake or reservoir. The following research question was formulated:

What is the potential of applying elevation models to monitor the volume levels of lakes and reservoirs, when replacing the flat elevations with extrapolated depths?

The case study comprised of two parts. First, the validation of the water level extraction was conducted for pre-selected lakes and reservoirs. The results showed an average RMSE of 4.10 [m]. When analysing the distribution of lakes and reservoirs data, the RMSE was centred at 1.27 [m] (NED and ALOS) and 3.70 [m] (SRTM). The comparison between the three considered elevation models, showed a minor improvement regarding the relative water level. At the same time, it demonstrated that the number of waterbodies that can be monitored increases when applying the developed tool.

The second part of the case study aimed at providing an insight in the potential of applying the DEM for estimating the volume variability. An analysis of the USGS in-situ data compared to the results, showed that the overall RMSE decreased for each considered model. From the same analysis, the relative time-series could be determined for each model i.e., in case the minimum amount of surface area was available and in case the water level variation was significantly noticeable.

The results from this work indicated the potential of the global elevation models to monitor the volume levels of lakes and reservoirs. The developed tool demonstrated that elevations can be extrapolated, which would fit a more realistic shape of the reservoir at areas where the bathymetry was flattened or not found.

Accurate information for extracting the water level and assessing the volume variability of lakes and reservoirs currently depends on extensive hydrographic surveys. This work provides guidelines for an alternative method: the Linear Bathymetry for Digital Elevation Models tool.

Table of contents

List of Figures

List of Tables

List of Acronyms

ALOS	Advanced Land Observation Satellite
ATLAS	Advanced Topographic Laser Altimeter System
CONUS	Continues USA
DEM	Digital elevation model
EGM96	Earth gravitational model 1996
FwDET	Floodwater Depth Estimation Tool
ICESat	Ice, Cloud, and Land Elevation Satellites
JRC	Joint Research Centre
L8	Landsat-8
LBDEM	Linear bathymetry for Digital Elevation Models
LiDAR	Light detection and Ranging
L&R	Lakes and Reservoirs
MDEM	MATLAB based Digital Elevation Model
MNDWI	Modified Normalized Difference Water Index
MODIS	Moderate Resolution Imaging Spectroradiometer
NAD83	North American Datum 1983
NED	USGS National Elevation Dataset
NDWI	Normalized Difference Water Index
NIR	Near Infrared
PRISM	Panchromatic Remote-sensing Instrument for Stereo Mapping
RADAR	Radio Detection and Ranging
RMSE	Root Mean Squared Error
S2	Sentinel-2
SA	Surface Area
SRTM	Shuttle RADAR Topography Mission
SWIR	Short-Wave Infrared
USGS	United States Geological Survey
V-A	Volume-Area
WL-A	Water Level-Area

1 Introduction

In the summer of 2021 seasonal floods hit large regions of Europe and China, where in some cases, even dams, and embankments, containing the water had to be blasted away to prevent damage to the population and region. Similar events happened in the USA, where extreme droughts caused the water level to drastically decline (Bernstein et al. 2021), most apparent in the Colorado River basin, experiencing the driest year in history. Hence stressing the need for real-time monitoring of the current water and volume level of the Lakes and Reservoirs (L&R) to prevent or predict future catastrophic events (Cretaux et al. (2015), Venot et al. (2012), Ballatore and Muhandiki (2001), Busker et al. (2019), Frappart (2018)).

Unfortunately, the monitoring data is slim or inconsistent as hydrographic surveys are expensive and time-consuming. Consequently, remote sensing is considered as an alternative (Abileah et al., 2011). Altimetry techniques are applied as an alternative to the high-resolution tide stations or bathymetric surveys. The downside of the instruments is that the low temporal resolution is relatively low. Furthermore, since flyovers can differ between 10 to 20 days apart, the water can also influence the retuning signal, causing an increased vertical error when apply for volume monitoring.

The recent high accuracy and high-resolution Digital Elevation Models (DEM) have shown to contain new opportunities (see e.g., Vanthof and Kelly, (2019)), since the terrain models are continuously updated by the respective agencies with the latest elevation data. Considering that with the recent gravity satellite missions, the global gravity models have increase in both spatial and vertical accuracy.

In combination with the high temporal multi-spectral imagery, implemented for estimating the water contour, the recent studies showed, that the elevation models can monitor the water level within a meter order of magnitude (Weekley and Li 2021, Avissee et al., 2017, Vantof and Kelly, (2019)). However, the study of Weekely et al., (2021) suggested that the available models were limited by the lack of bathymetry data.

The water column prohibits the ability of constructing the waterbed, due to the loss of the returning signal. Hence instead of including the noise elevations, the surfaces are given one single elevation value, representing the last determined depth at the water level. In Figure 1 is the flat-elevation phenomenon depicted, portraying the bathymetry on the right, while showing the same reservoir of an older DEM. The black region in the left depiction of the reservoirs, portrays the flattened area where at the moment of construction, the water level was currently at.

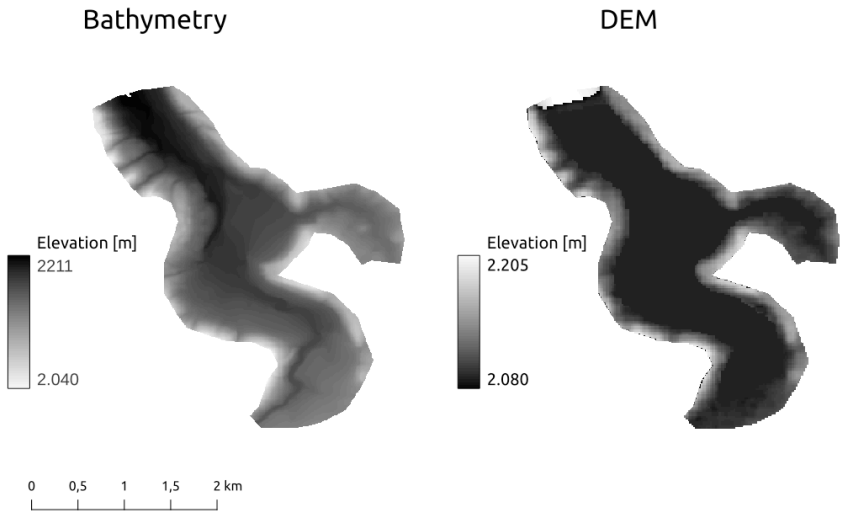

Figure 1 Example of the flattened elevation, where the bathymetry(left) and the DEM (right) of the Ridgeway reservoir (Colorado, USA) is portrayed

In comparison between the bathymetry and the DEM on the left, the region that is located at the waterbed is flattened. Therefore, the water level will not be estimated when the surface area declines. Also, the volume level will be different relative to the bathymetry output, as the variation will not be seen in the time series.

Thus, when analysing the results and limitations found in literature, on applying the elevation models to monitor water and volume levels, the main innovation is the replacement of flattened surfaces by extrapolated depths. Direct implementation of the global available elevation models in combination with the multi-spectral imagery is currently not considered for volume variability.

1.1 Research objective

The research objective can be formulated as follows:

- The development of an algorithm for replacing the flattened pixels in DEM, with linear extrapolated elevations based on the slope. The different datasets for this study will be collected through the Google Earth Engine data catalogue, to supply a tool based on open-accessible datasets.

- Provide an insight in the applicability of global / local elevation models for the estimation of the volume level. This study will demonstrate the effect of using models with different spatial resolutions, which will be compared against the water-level and the volume time series data from the United States Geological Survey (USGS).

- Demonstrating the potential of the elevation models for finding the water level aimed at monitoring the effects of water-level change smaller L&R as well.

1.2 Area of interest

This study defines L&R according to Hayes et al., (2017) and Liebe et al., (2005) as water bodies that are either valley-dammed, at the bank side of rivers or man-made. Smaller L&R for this study and in line with the study of Vanthof and Kelly, (2019), being between 0.1 and 5 km^2, so the assumption can be made that the spatial variation in the water-level is neglectable.

The aim of this study is to investigate the effect of the small reservoirs; therefore, the number of available sites is limited. The USGS provides a large database of the in-situ datasets that are publicly available. The selection-procedure consist of three steps, which are elaborated on below.

First the L&R are filtered based on the maximum extent, determined by the water-occurrence provided by the Joint Research Centre (JRC). Followed by a comparison with the lowest found elevation in the different DEM and the maximum found in-situ water level. Favouring L&R that can potentially have bathymetry (like the test reservoir) or a sufficient usable for implementation of the tool. The last step was to filter the reservoirs based on the volume data was monitored in this reservoir in the set period (2016 to 2021).

	Total L&R	Smaller L&R	Water-level	Volume-level
Num. reservoir	537	193	88	30

Table 1 Selection of the Lakes and Reservoirs for the implementation of the DEM water level and volume monitoring

The results of these filtering steps are shown in Figure 2, where the number of reservoirs is given per selection step. Please note that the USGS also monitors waterbodies in Porto Rico and Alaska. These were not considered for this study, therefore only focusing on the Continues USA (CONUS).

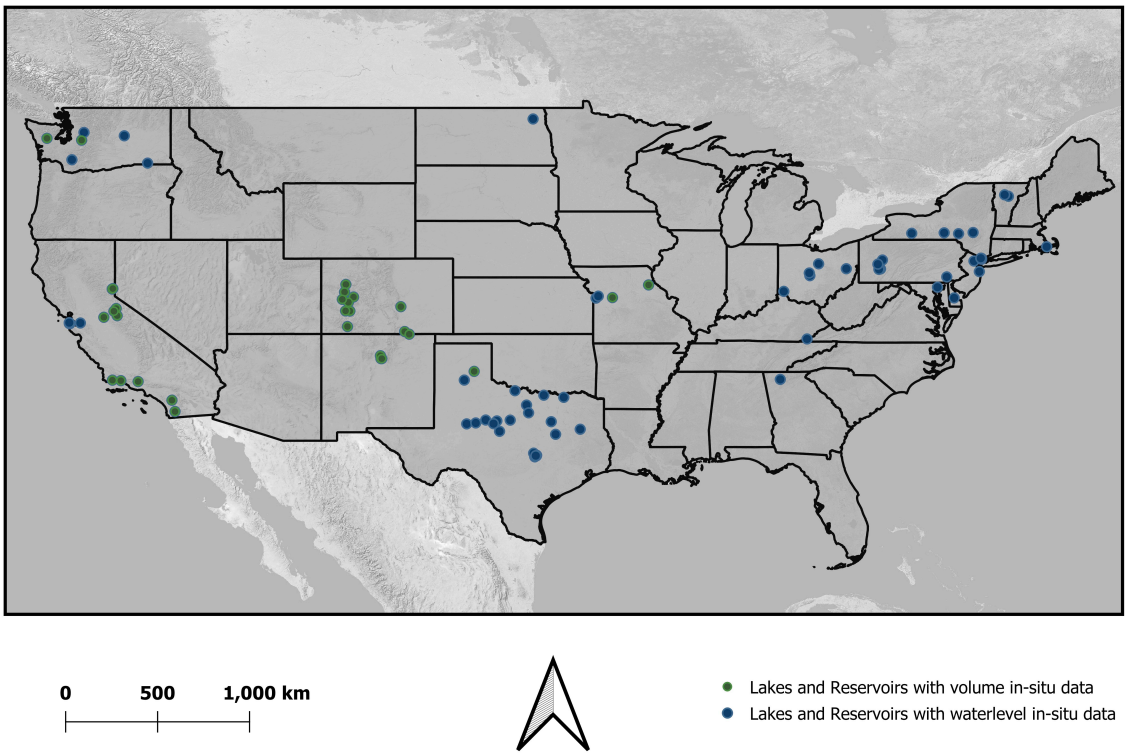

Figure 2 Locations of the Lakes and reservoirs in the USA that were considered for the monitoring the volume and water level time series.

1.3 Research question

From the objectives the following main research question is formulated:

What is the potential of applying elevation models to monitor the volume variability of lakes and reservoirs, when replacing the flat elevations with extrapolated depths?

When applying the developed tool for extrapolating elevations at the flattened pixels, an insight is provided for determination of the water level and volume variability in periods where the surface area has declined into the flattened region. Showing if global elevation models can serve as an alternative to the current method of estimating the volume level of lakes and reservoirs.

To support the main research-question the following sub-questions are formulated, which describes a small subsection of the research:

- What is the effect of using lower spatial resolution multi-spectral data for estimation of the water level, used for water level monitoring?

  The study of Deng et al., (2020) suggested that the Sentinel-2 imagery data can be considered instead of the frequently applied Landsat-8 data. The effect will be that higher spatial and temporal constructed binary land/water images are used, therefore strengthening the water level estimation process.

- What is the effect of using lower spatial resolution DEM for the extrapolation of the elevations?

  For the area of interest three elevation models were considered, which are constructed with different techniques, resolutions and at different moments in time. Considering for a global implementation not every elevation model will be available, therefore supplying knowledge regarding the utilization of the tool in different situations.

- What are the benefits of using the least flattened DEM in-order to improve the estimation of volume variations?
-

  The study of Weekley and Li (2021) suggested that the flattened pixels prohibit the ability to successfully determine the water-level. Especially when the surface water declined to fully covered these flat regions. Hence when selecting the elevation model based on the lowest amount flat pixels, benefit could be seen in the water-level monitoring. Since the DEM with the highest like amount of bathymetry would be favoured.

- What is the effect of extrapolating elevations in-order to estimate the volume level?

  The estimation of the volume time-series is also limited by the flattened pixels, frequently located at regions where the water occurrence is high. Hence the implementation of the developed tool to simulated depths at these regions can give an insight in the potential of the elevation model for volume estimation. As now a more realistic model is constructed and where the flatted regions have a reduced influence on the water level selection.

1.5 Research novelty

In this work for the first-time linear extrapolation will be implemented to determine depths at global elevation models that were removed at locations where the bathymetry was not found. The tool, when successful, will increase the number of L&R that can be monitored from space, with a high temporal resolution achieved by, for instance, the multi-spectral imagery data of S2. As the tool will be tested on openly accessible data, the tool is applicable for global implementation.

The results at the area of interest will contribute to the understanding of smaller L&R, which are less likely to be monitored by gauged systems. Therefore, this work supports the development of water level and volume monitoring based on remote sensing instruments.

1.6 Thesis outline

The thesis is outlined as follows; in Chapter 2 the literature study is provided. In this chapter the techniques are briefly discussed how the DEMs' are constructed as well as the latest algorithms that are used for flat pixel replacement and the current state for volume and water-levels monitoring. In Chapter 3, is the linear extrapolation tool is analysed including the foundation, limitations, and visualisation of the resulting DEM. In Chapter 4, the method is discussed, while focusing on the newly added steps that were applied for the estimation of the results in the area of interest. Chapter 4 also reviews the datasets that will be applied in the method. Chapter 5 will demonstrate the results found in the area of interest while implementing the LBDEM tool for water level and volume determination. Chapter 6 focuses on the discussion of the results, followed by the conclusion in Chapter 7 and recommendations.

2 Literature review

2.1 Review of the considered digital elevation models construction techniques

In this subsection the acquisition methods of the different elevation models are discussed. The following techniques used to build the considered elevation models are RADAR (§2.1.1), LiDAR (§2.1.2) and Stereoscopy (§2.1.3). Each method is briefly discussed, including with the accompanied limitations and vertical accuracy levels.

2.1.1 DEM constructed with RADAR

The Radio Detection and Ranging (RADAR) acquisition method, is frequently applied in the development of elevation models (Colins et al., (2015)). As the system transmits radio signals, the backscatter will not be hindered by clouds or vegetation (Tarpanelli et al. 2019, Amitrano et al., 2014). Therefore, considered to be favourable method for the construction elevation models. While also having the capability to potentially penetrate the water column up to a certain depth.

To visualise the RADAR acquisition technique, two methods are depicted in Figure 3, showing two different instruments: TanDEM-x (left) and SRTM (right).

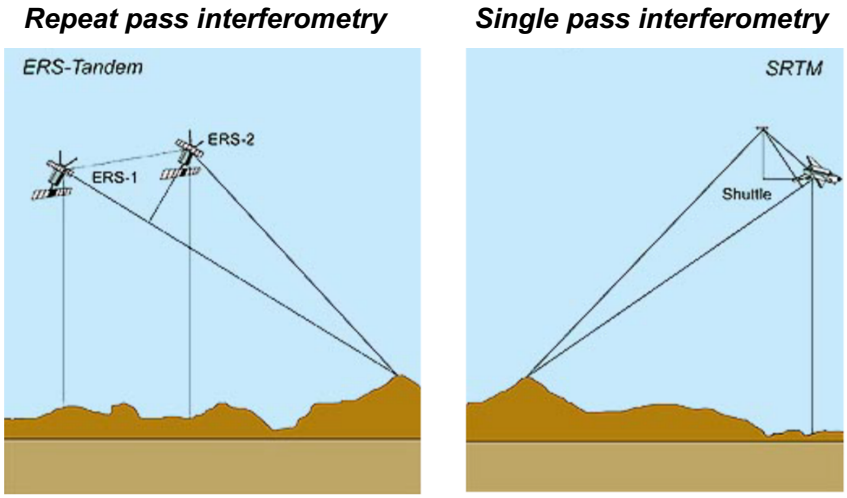

Figure 3 Two examples of DEM construction by use of RADAR instruments, were the Repeat Pass (left) and the single pass (right) interferometry is given

The repeat pass interferometry (left) consists of two satellites that create two backscatter images in between a lag time is present. This lag-time caused the ERS-TanDEM mission to be affected by variations of for instance wind, influencing the correlation between the two images that are combined for the creation of the elevation model.

The right depiction of Figure 3 shows the single pass interferometry, which uses two backscatter images created at the same time. An example of the method is Shuttle RADAR Topography Mission (SRTM), where the extended antenna from the shuttle was used to create the second image. In both cases a coherence map is extracted from between the two images, where the elevations can be deducted.

Using RADAR shown in the examples, have different limitation present that influence the final elevations. For instance, the speckle noise arises from the coherence maps, creating a spatial variability between the two images, seen as a random bias. The origin of this problem is found at the variability in reflectance of the surface over a flat area (Rodriguez et al., 2006, Shawky et al., 2006 and Shawky et al., 2019). Therefore, enlarging the travel path of the pulse, and thus introducing a vertical error in the elevation that are distinguished as noise.

Likewise, the shift in average elevation within a large region can be seen as the absolute bias. To correct for the shift in elevation, ground control points are needed for collecting the reference heights. Which remains difficult in some regions, resulting that the error tends to be larger in regions were these validation points are not available in the high-quality that is required.

The limitations from the RADAR based technique led to an elevation error of 6 and 12 [m] for the SRTM elevation model in flat areas. When the gradient increases, the error increases slightly for SRTM (Uuemaa et al., 2020). The same study concluded that the error for TanDEM-X was 8.25 to 10.25 [m] for slopes with a gradient lower than 5°. While having a respective spatial resolution of 30 [m] for SRTM and 90 [m] for TanDEM-X.

Important to consider that the resolution does not take the flat area at water regions in consideration. The effect of the flat elevations found for this technique is shown in Figure 4. Here a simulated reservoir was filled for water levels, portraying the effect of the backscatter affected by water in the elevation models (Amitrano et al., (2014)).

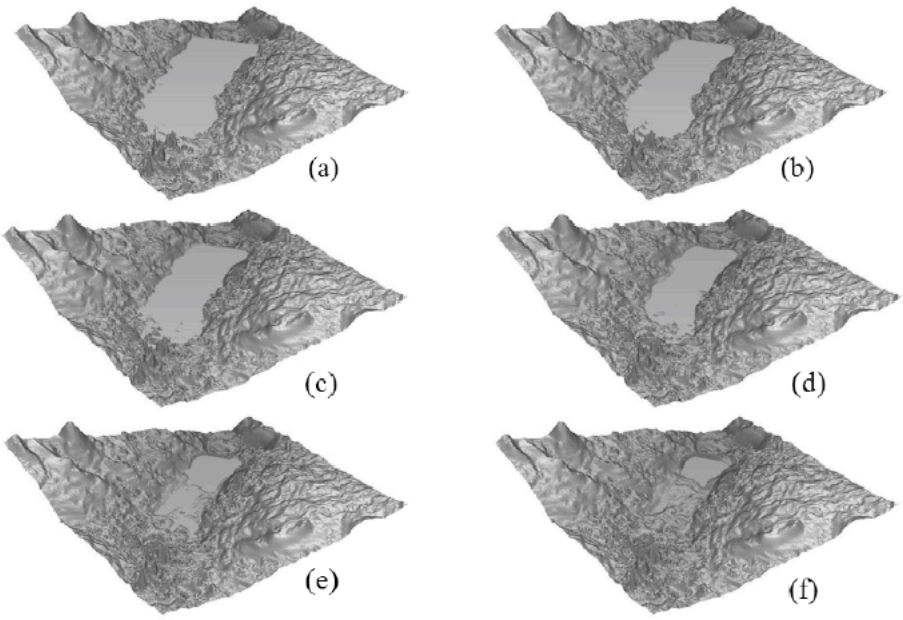

Figure 4 Simulation of having different water levels when the DEM was constructed (taken form Amitrano et al., 2014).

The backscatter is not returning when the water level increases. Hence the waterbed is secluded from the underlying bottom. The reason for this is that in general transmitted signals cannot fully penetrate the water column. As a results at a certain depth, the pulses will be reflected away or returned at lower decibel levels, so the original waterbed ripples are removed out or, in the case of SRTM, flattened (Sanborn, 2018).

2.1.2 DEM constructed with stereoscopy

Stereoscopy is the second technique considered for this study. The method uses two images are taken at a fixed time apart. The resulting images are then matched, to identify corresponding features, by finding overlapping pixels. Vertical elevation can be deducted from the match images, taken that there is a minor difference in overlap due to the geometry and the distortion and that the location the satellite is known.

To visualise the stereoscopy technique, the following representation is given in Figure 5, where two satellites are portrayed measuring over one ground feature.

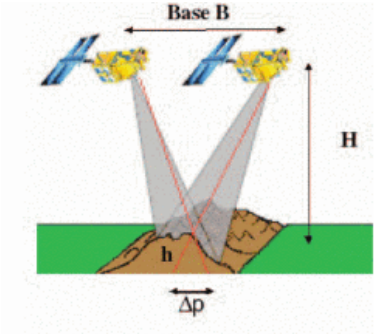

Figure 5 An example of the SPOT-5 acquisition method using the stereoscopy

Here *H* represents the height/elevation between the satellite and the reference frame, *h* the orthometric height, and *B* the distance between the two satellites. The shift between the taken images is given in the resulting Δp. Hence the following equation is given for computing the elevation:

$$\Delta p = \frac{B}{H} \cdot h \rightarrow H = \frac{B}{\Delta p} \cdot h \quad (1)$$

An example of Stereoscopy method is the Panchromatic Remote-sensing Instrument for Stereo Mapping (PRISM). This instrument has a panchromatic radiometer, which includes 3 independent optical systems (nadir, forward and backward) that constructs a stereoscopic image that can be utilised for the construction of elevation models (Stéphane and Christophe, (2009)) For example, the SPOT-5 panchromatic mission consists of two satellites that are in different orbits. Therefore, a significant time delay occurs between the images taken by the different satellites of this mission. Causing an increased sensitivity by clouds and landscape evolution in the resulting elevation model.

The resulting data from PRISM was utilised to construct the Advanced Land Observation Satellite (ALOS) (Tadono et al., (2014)). Several limitations for this mission are that strip noise and random bias occur, as well as that the signal cannot penetrate water. This is because the constructed images are depending on the returning light, which at lower water depths will be decreased or absorbed by the water. As a result, ALOS elevation model has a vertical RMSE was below 5 [m] for flat regions and increases to 12 and 14 [m] in regions with higher and complex slopes (Uuemaa et al., (2020), Takaku et al., (2020) and Santillan and Makinano-Santillan, (2016)), where the elevations underwater level is removed/flattened.

2.1.3 DEM constructed with LiDAR

As an alternative to the earlier discussed techniques, the Light Detection and Ranging (LiDAR) acquisition method is considered for this study. LiDAR can be mounted as either an air or space borne instrument, and is used to create elevation models, or validate others (Yamazaki et al., (2017), AHN (2020), Gesch et al., (2002)).

Although airborne LiDAR produces beneficially dense models, with spatial resolutions of 0.5 [m], those are a limitation on its own. For data-size purposes, airborne LiDAR has to be divided into small areas, and is available in certain countries and regions that dedicated missions (AHN (2020), Fouladine et al., (2019)),

Therefore, the space borne Ice, Cloud, and Land Elevation Satellites (ICEsat) missions are also considered for the validation of elevation models, due to the potential shown in the recent studies (Parrish et al., (2019)). The ICEsat-2 mission is equipped with the Advanced Topographic Laser Altimeter System (ATLAS (Neumann et al., (2019)). The beams can penetrate the water column (up to 40m in clear water (Parrish et al., (2019)). Therefore, increasing the likelihood of capturing the surface of the waterbodies. However, due to the relative smaller footprint of the beams, elevations can only monitor at pre-set intervals Yamazaki et al., (2017), When the ICEsat-2 data is used for estimating the water-level and submerged bathymetry at clear-water occasions, the vertical RMSE was estimated to be 0.43m to 0.60m after refraction corrections.

A limitation found in the ICESat data is that the footprint has a size of 17m, while having the photons lines 3.3km apart from each other. Therefore, reservoirs that are in between those lines could easily be missed when implementing this method for monitoring the water level.

Also like the earlier methods, the LiDAR data is influenced by the absolute error and the effects caused by the tree height bias. The bias is affected by the fact that trees are reflectors for both LiDAR, RADAR, and Stereoscopy (i.e., PRISM). Therefore, when the waterline is located near or directly under trees, a vertical error is introduced in the elevation. Here a difference per model can be seen, as some elevation models are created over a barren earth (e.g., trees are removed) or represent the surface including the different features.

In some cases, the elevation model is constructed while using a combination of the previously mentioned techniques. For instance, the USGS National Elevation Dataset (NED) is the primary DEM of the CONUS, Alaska, Hawaii, and the island territories. This elevation model is a derived product from different altimetry sources, that are processed to a common coordinate system and vertical unit.

The accuracy assessment of this model conducted by the USGS, estimated that the overall vertical error was 2.44 [m] for the continues USA (Gesch et al., (2002)). An increase in the error can be noticed at elevations that are located at high gradients, which is true for all development techniques.

2.2 Review of the available bathymetry algorithms

The literature showed that there are different algorithms available that constructed depths when working with elevation models. Two of the latest algorithms dating from 2019 were considered for this study, being the, MATLAB based Digital Elevation model (§2.2.1) and the Floodwater Depth Estimation tool (§2.2.2).

2.2.1 MATLAB based Digital Elevation model

The MATLAB Digital elevation model (MDEM) is an algorithm that replaces flattened pixels with a bathymetry, based on the linear variation between the in- and out-flow of the water stream (Pan et al., (2019)). The 8x8 pixels search-kernel is used for determining which pixels are considered flat and the in-and-out flow elevation. This process is repeated multiple times, until no flat pixels are classified, therefore resulting in a computationally heavy algorithm (Pan et al., (2019)).

To visualise the resulting bathymetry, when applying MDEM, examples of the ALOS and SRTM elevation models are given for the Ridgeway reservoir (Colorado, USA). In the left depiction the NED model is given, which includes the likely bathymetry of the reservoir. Therefore, can be served as a comparison of the achieved results.

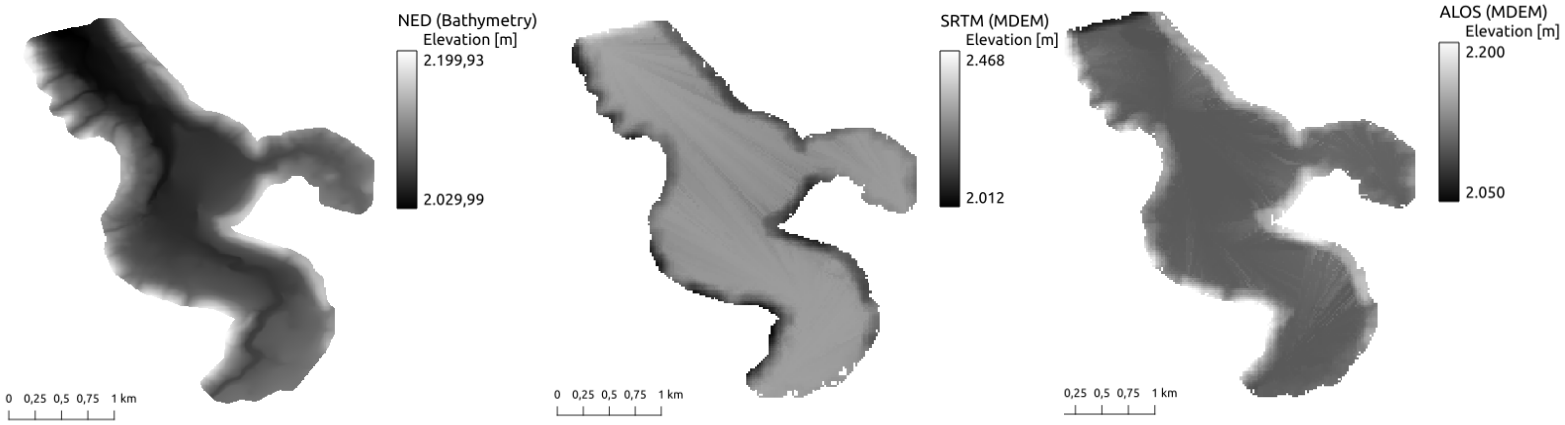

Figure 6 Visualization of the MDEM result, were the bathymetry (left) and the SRTM (middle) and ALOS (right) are given

The pattern, at which the in-and-out flow pixels are determined, can be seen by the lines drawn to north of the reservoir of the middle figure. The newly created surface is extrapolated to the lowest elevation, therefore creating a cone shape in the direction of the out-flow region of the reservoir. However, the resulting waterbed does not resemble the same depth of the NED model. Implying that the bathymetry determined by using MDEM projects the newly found depths over the flat area. Hence, the main limitation of MDEM for water-level and volume monitoring is that the surface is projected over the flat pixels. Causing the depth to decrease, that the volume variability falsely becomes small or neglectable.

Thus, MDEM would lead to a fewer number of flat pixels and thus the region for which the water level can be determined have decreased. Monitoring of the volume would therefore also not be possible or lead to false outcomes when the surface is projected over the flat pixels.

2.2.2 Floodwater Depth Estimation Tool

The second algorithm is the Floodwater Depth Estimation tool (FwDET), designed to determine depths at areas where the water has flooded a specific region. The basis of FwDET is to compute depths based on the inundation region, while subtracting the (flood)water from the topographic elevation determined from the selected DEM using nearest neighbour method (Cohen et al., (2019)) Therefore, taken the spatial water level variation into consideration that can be present at L&R.

An example is given in Figure 7 of the resulting elevations using the FwDET algorithm. Here the SRTM depiction of the Ridgway reservoir is shown, since this DEM had the highest number of flat pixels. In red is the shape of the reservoir is given for illustration purposes.

Figure 7 Results of the Floodwater Depth Estimation tool, were the SRTM was used to illustrated the effect on the elevations

Striking is that the depiction is relatively coarse in comparison to the original DEM (see Figure 7), as the algorithm has extrapolated the elevations linear to the centre of the reservoir. The nearest neighbour selection caused the reservoir to select the closest elevation, therefore adopting relative high elevation values creating the coarse DEM of the reservoir. Such a coarse DEM would not perform well for estimation of bathymetry.

The second reason that FwDET would not operate sufficiently for the estimation of the bathymetry of the L&R, is the lack of information at the flat pixels. The algorithm was originally built to compute the water depths at regions that are flooded, which in does not include flatted elevations. Thus, using this depth algorithm can only be considered when working with bathymetry including data at larger L&R.

2.3 Review of the currently suggested workflow

The use of elevation models has been studied frequently for extracting the water level and volume variation (Weekley and Li (2021), Bonnema and Hossain (2017), Deng et al., (2020), Zhang et al., (2016)) suggesting a processing pipeline that can be implemented for the monitoring of the water level for L&R. In Figure 8 are the steps given, which are commonly applied by the literature.

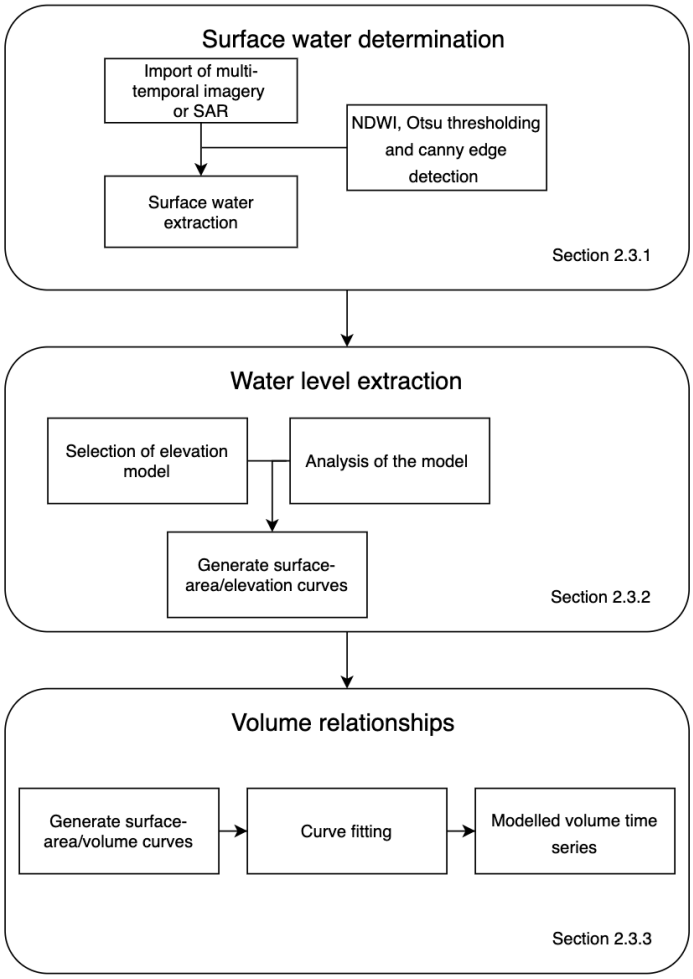

Figure 8 A summary of the suggested workflow by the literature for estimating the water level and volume time series.

Three different phases can be distinguished for the suggested workflow: the surface water extraction (1), the water level estimation (2) and the volume estimation (3).

2.3.1 The extraction of the surface water contour

The first step in determining the water-level, is estimating the contour between the water and land. The normalised difference water index (NDWI) (Mcfeeters (1996)) or the Modified Normalized Difference Water Index (MNDWI) (Xu (2006)) are frequently applied, formulated as follows:

$$\mathrm{NDWI} = \frac{\mathrm{Green}_{\{\mathrm{band}\}} - \mathrm{NIR}_{\{\mathrm{band}\}}}{\mathrm{Green}_{\{\mathrm{band}\}} + \mathrm{NIR}_{\{\mathrm{band}\}}} \tag{2.1}$$

$$\mathrm{MNDWI} = \frac{\{\mathrm{Green}_{\{\mathrm{band}\}} - \mathrm{SWIR}_{\{\mathrm{band}\}}\}}{\{\mathrm{Green}_{\{\mathrm{band}\}} + \mathrm{SWIR}_{\{\mathrm{band}\}}\}} \tag{2.2}$$

Note that the SWIR (eq. 2.1) and NIR (eq. 2.2) are the reflectance collected in the short-wave infrared and near infrared band. Both equations are based on multi-spectral imagery data and the fact that water significantly absorbs most of the infrared radiation (Mcfeeters (1996)).

This absorption of infrared radiation by water typically distinguishes water from land. However, this is not always the case (Donchyts et al., (2016)), therefore, to improve the classification, the Otsu thresholding is applied (Ji et al., (2009), Otsu (1979)).

Otsu thresholding uses using the fisher's linear discriminant analysis, to compute the optimal fitted threshold by dissecting the image in multiple classes. The most basic form of this method is by classifying an image into two classes (e.g., land and water). This can be achieved by analysing the histogram of the pixel distribution of resulting NDWI values (please note that this distribution represents a bivariate distribution). An example of such classification is given in Figure 9 for the Crawford reservoir (Colorado, USA). Here the NDWI pixel histogram is portrayed, where the red line shows the Otsu threshold.

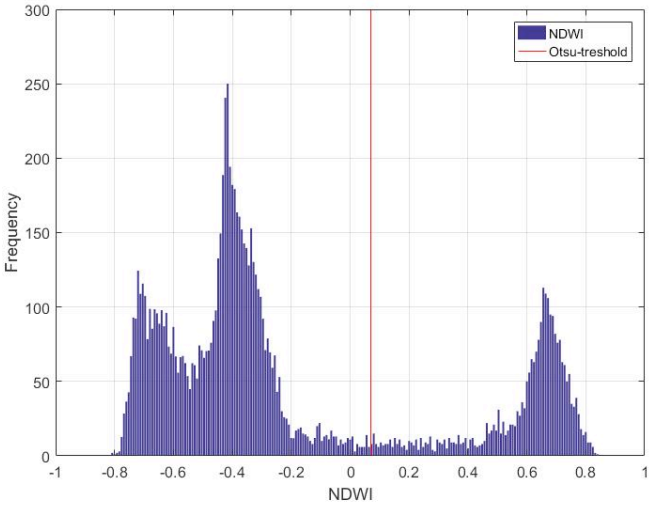

Figure 9 Example of the NDWI – Otsu thresholding for the Crawford reservoir (Colorado, USA)

So, considering NDWI values of Figure 9, the threshold is determined at 0.06 rather than 0, which is normally expected when distinguishing land and water NDWI values. Since the distribution of the water-pixels is more concentrated between 0.6 and 0.8, with the Otsu threshold these will all be classified as water, whereas anything with a NDWI value below 0.06 will be classified as land.

The result is a contour between the binary water/land classes. Then the use of the canny edge detection method (Canny (1986)) is applied. The method follows on the following five steps: (1) images are smoothed by use of a Gaussian kernel (hence removing high-frequency noise), (2) intensity gradients are computed, (3) to remove spurious edges a non-maximum suppression is applied, (4) for finding the potential edge double thresholds are computed and finally (5) the edges that are classified as weak or have no connection are suppressed.

The processed multi-spectral images are provided in two types: top of atmosphere reflection (TOA) and surface reflection (SR). The images from the former are supplied without the atmospheric corrections (i.e., aerosol anomalies). Whilst the SR images are supplied with the appropriate corrections, hence, portraying images that have clearer surface reflections. However, as the goal of this study is to determine the contrast between land and water, higher wavelengths can be utilised, which are less affected by the atmospheric parameters. Therefore, the TOA images can also be used for determining the surface water extend (Donchyts et al., (2016)).

The limitations connected to the suggested steps of this phase are related to the multi-spectral imagery data, as this sensor measures the earth within the electromagnetic spectrum producing optical images. Therefore, different anomalies can potentially limit the performance of the NDWI/Otsu method by either natural and/or technical conditions. For example, the surface water extent of reservoirs and lakes might be detected wrongly as they are prone to current weather conditions like snow or ice. Likewise different cloud types can limit the ability to measure the underlying surface Aerosols may also cause anomalies by causing atmospheric transmission losses in different bands. Finally, the presence of shadows (i.e., from mountains), can result in gabs or black pixels that are classified as land by the NDWI/Otsu method.

2.3.2 The estimation of the water level

Next, the water-level can be determined based on the water surface extent. Here an altimeter can be utilised to determine the water elevation by use of radar (Pham et al., 2017 and Piptone et al., 2018) or LiDAR is applied to determine water level of the lakes and reservoirs (Parrish et al.., 2019, Ma et al., 2020 and Xu et al., 2020).

Alternatively, the studies showed that the use of digital elevation models (DEM) can be used for estimating the water level (Weekley and Li., (2021), Vanthof and Kelly, (2019), Zhang et al., (2016), Avisse et al., (2017)). Currently the application of DEM has been preliminary tested as a tool to deduct the water level from different L&R. For instance, the study of Weekley and Li., (2021) demonstrated, that when selecting the DEM with the least flattened surface an improvement a RMSE of 2.41 [m] was found between the USGS data and the estimate time series (while using only clear images).

To reduce noise found in the estimated water level a smoothing filter was frequently applied, based on the 1st, 2nd and/or 3rd polynomial hypsometric relationship (i.e., surface area extent and water level). An illustration of this relationship is given in Figure 10, portraying the Clinton Lakes (Kansas USA) the surface area [km^2] in relation to the water elevation [m] (taken from Weekley and Li., 2021)

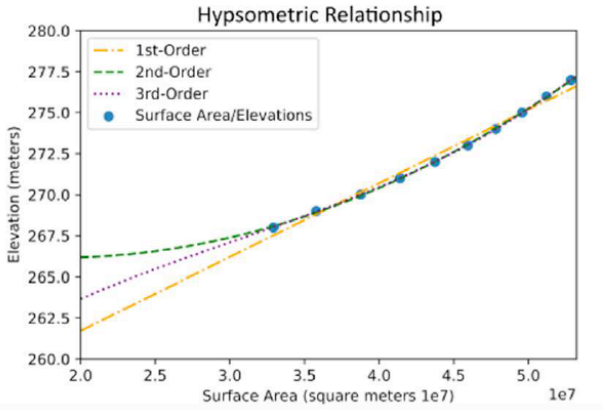

Figure 10 Example of the hypsometric relationship for smoothing the elevations, based on the surface water time series (taken from Weekley and Li, (2021))

The curve shows the relationship between the water level and surface area described by either the linear and/or 2nd/3rd polynomial. Hence, when data differs from this pattern, the curve can serve as a smoothing method for the estimation of the water level time series. The study of Weekly et al., 2021 concluded, that based on the results, the 2nd polynomial was the optimal choice, were an increase of the water level RMSE was found of 2.41 [m].

However, one of the limitations of this using the hypsometric relationship for noise reduction in the water elevation time series, is the fact that the surface area can change position over time, while remaining constant in size. Examples of this phenomena are the area is altered by the wind, or by introducing man-made constructions resulting in a change waterflow.

This phenomenon is given in Figure 11, portraying two moments in time are depicted, representing artistic surface interpretation of a circular reservoir.

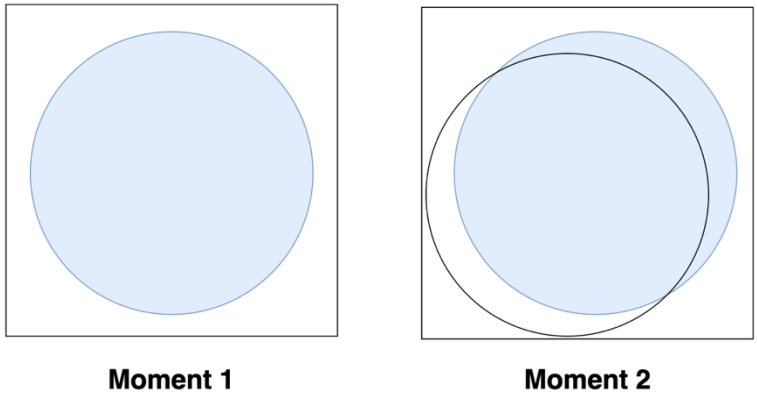

Figure 11 Example of the limitations for using the surface water as a smoothing filter

The example depicts that the surface changed position, while the water level can vary. However, this will introduce an error when considering the hypsometric relationship, as multiple elevations will have a constant area. Therefore, when using the 1st or 2nd polynomial (e.g., Zhang et al., (2014), Weekley and Li, (2021)), data could be distinguished as noise, when creating the smoothing water level curve.

2.3.3 The estimation of the volume time series

The final phase, in when the study considers estimating the volume of L&R, is the construction of the Volume-Area relationship. For instance, considering the simplest form of a reservoir, i.e., the pyramid shaped, the following power law equation (Liebe et al., (2005))

$$V = a \cdot A^b \quad (2.3)$$

Here *V* represents the volume of the L&R, *A* is the surface area, *a* is the scaling coefficient and *b* is the indication of the decay or growth of the model. Equation 2.3 is used in studies to model the reservoir based on surface area and in-situ volume values. However, each waterbody has respective different *a* and *b* of Equation 2.3. For instance, small (and medium) sized reservoirs commonly have one or two inflows (Diekkrüger and Liebe (2002)) or are located upstream, which causes enough variation in the elevation to facilitate dams. Therefore, having different effects on the change in surface area and thus changes the factors *a* and *b* of Equation 2.3.

The equation 2.3 or the bathymetry extracted from TanDEM-X self-constructed elevation models, is used to create the depth-capacity curves, where the water level is expressed against the volume (Peng (2006), Deng et al., (2020), Gal et al., (2016), Vanthof and Kelly (2019), Avisse et al., (2014), Hang (2016)). The correlation between the volume found by models is presented with high correlation coefficients (typically >0.8).

The Vanthof and Kelly (2019) study, concluded that working with the power relationship, the volume levels of small L&R were determined using the TanDEM-X model to be between 6% and 8% of the absolute volume range. However, those results were found for basins that had a water level lower than 1.5m, suggesting that in other cases bathymetry data should still be considered.

The limitation that can influence the V-A relationship, are that the rivers increase or decreases due to sand transportation downstream (Wisser et al., 2013). This feature is important due to the fact, that upon arrival in the reservoir the current drops significantly, hence the sand will set down. Changing the shape over the waterbed over time. These shapes influence the outcome of the correlation equation, as the surface area is variation differently for each L&R.

3 Linear extrapolation tool

Chapter 3 comprise of the construction of the linear extrapolation tool, where the background is discussed (§3.1) and the basis of the method including the limitations (§3.2).

3.1 Background

The flattened pixels in the elevation models limit the ability to estimate the water-level and volume time series. The Linear Bathymetry for Digital Elevation Models (LBDEM) is based on the "half pyramid" system that represents a L&R in the simplest form (Liebe et al., (2005)), in line with the constructed fundamentals of the MDEM and FwDET algorithms. To illustrate the pyramid shape, Figure 12 is given, where an artistic interpretation is shown of the shape of the waterbody.

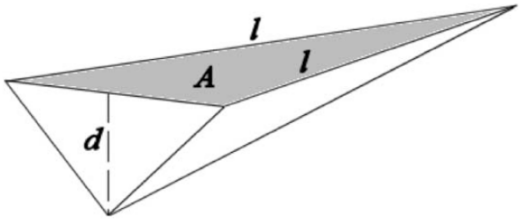

Figure 12 The fundamental pyramid shape that serve as the basis of the developed tool

Here 'd' represents the depth of the reservoir, which becomes deeper at the centre of the surface area (given as A). Also, the shape takes into consideration that the reservoir or lake is fed by a river or other water source. Thus, taking the linear approach of the MDEM and FwDET algorithms for extrapolating the DEM elevations.

3.2 Design and visualisation

To construct the pyramid shape, the tool uses two kernels to iterate over the flat classified pixels. Each kernel, visualised in Figure 13, has a different shape. The first kernel comprises of a 3x3 pixel gird, while the second larger kernel uses a 5x5 kernel.

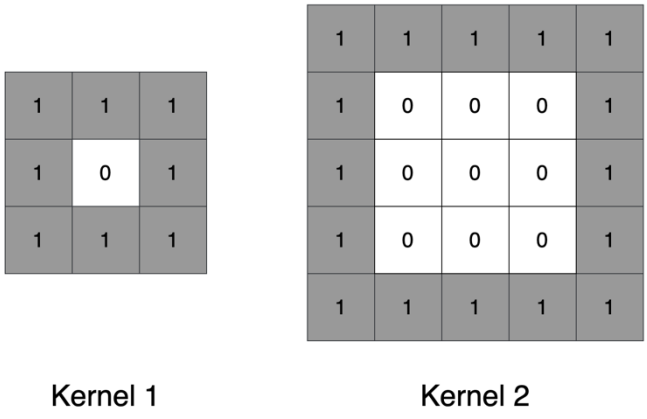

Figure 13 Kernels that are applied for the LBDEM tool

Depending on the scale of the DEM, the size of the kernels can change. For instance, when using a model with a scale of 25m the small kernel will be 75x75m, whilst a model that has a 1m resolution has a 3x3m size. The centre of the kernel is initially left empty, as the outer pixels contain the information that are used for determining the linear change in elevation. Please note that when working with the two kernels, the flat elevation-pixels are removed from the model and do not influence the linear change.

Subtracting the average elevation of each kernel from each other will give the mean slope for centre pixel. This mean difference can then be subtracted from the centre pixel, creating a new elevation that is linear extrapolated.

The extrapolation process can be repeated until the complete flattened surface includes simulated depths. This study utilised 40 iterations for simulating the elevations of the flattened pixels. When all the elevations are filled the tool will stop, therefore not altering the surface that is extrapolated.

Furthermore, two limit-thresholds are constructed to stop the tool when the slope is too steep. Since high gradients can cause the elevation difference to be relativity high, when not stopped, create depths that potentially go to infinity. The second threshold is created to limit the elevations to go higher than the flatted surface. Therefore, when a small difference in elevation is found, the extrapolation process will create false bathymetry features.

In Figure 14 the effect is given of applying LBDEM for the SRTM elevation model of the Ridgway reservoir, here the minimum threshold was set at 30m (LBDEM-30). The dark blue elevations in the original DEM depiction, represent the flat elevations at 2091 [m].

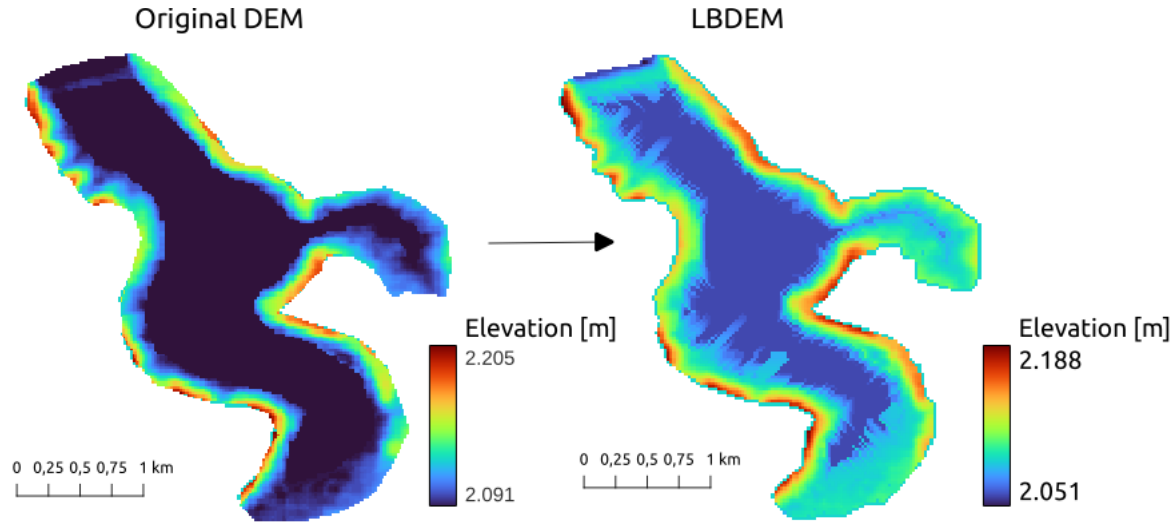

Figure 14 The effect of applying the LBDEM model on the Ridgway reservoir (Colorado, USA), while using the STRM DEM (NASADEM30).

The flattened surface of SRTM in Figure 14 is lowered with 30m. Where a larger region of the DEM can be now potentially be implemented for the estimation of the water level in the reservoir. In comparison to MDEM, the volume time series can be estimated by creating a bathymetry to replace the flat elevations, instead of projecting a pattern-based waterbed over the depths.

To compare the effects of LBDEM applied for the SRTM, the bathymetry of the Ridgway reservoir was subtracted from the resulting DEM. In Figure 15 the results given, showing three maximum depth thresholds given. Here red portrays the elevations that are respectively higher and lower than the original bathymetry, while green shows the depths within a threshold of +/- 5m.

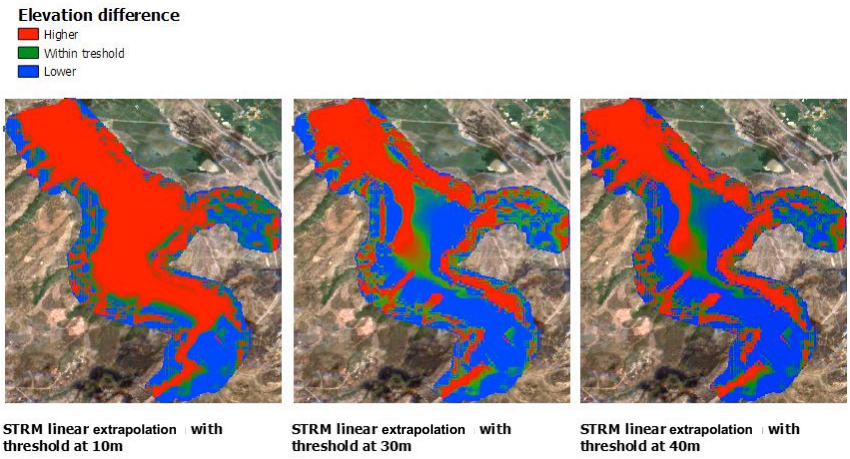

Figure 15 Effects of using different thresholds for the extrapolation of the elevations in the SRTM -DEM for Ridgeway (Colorado, USA).

The main limitations of LBDEM can be seen at all three depictions, as the bathymetry is not found in either result. Features that are located at for instance the centre of a L&R will not be constructed when using the LBDEM tool. Thus, the reader should consider that the tool aims only to support the estimation of the water level and volume level, and not replace hydrographic surveys.

4 Method and Data

Chapter 4 focuses on the method applied for the determination of the water and volume levels (§4.1), here each added step of to the suggested workflow in comparison to the literature will be elaborated. Followed by the applied datasets that were considered for the analysis of the LBDEM method (§4.2). The case study setup is briefly discussed in §4.3.

4.1 Method

The applied method is given in the flowchart of Figure 16. Where each step is visualised for the Ridgeway reservoir (Colorado, USA), showing the applied 3 suggested steps by the literature: the estimation of the surface water contour (1), the extraction of the water-level (2) and the volume determination (3).

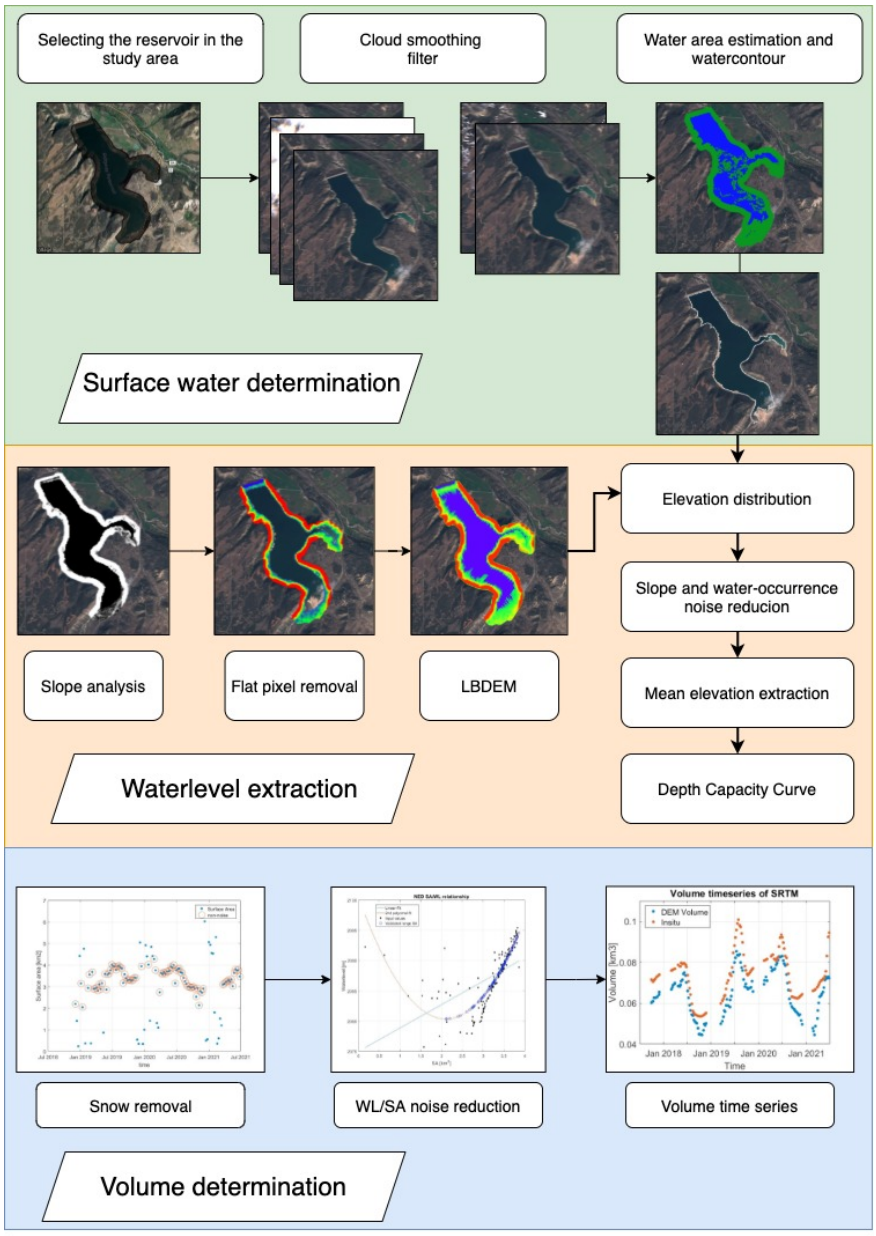

Figure 16 Applied method of the case study in the area of interest

When comparing the applied method with the suggestions of the literature, the main difference is the application of the LBDEM tool. LBDEM was implemented prior to the extraction of the water level and determination of the volume time series. To adjust for the limitations posed by the suggested method, the added noise reductions are discussed for each phase in the workflow.

4.1.1 Water contour determination

Cloud temporal smoothing filter

The QA60-band filter uses the 60 [m] spatial resolution band supplied with the S2 data to classify images containing more significant portions of dense clouds. The Cloud probability filter is an image-collection computed by the Sentinel 2-cloud-detector library, delivering a 10 [m] resolution cloud-mask probability image. Each pixel will have a value between 0 and 100, representing the chance that a cloud is presented. This study utilises the max cloud probability of 60% with a threshold set at 50%. Hence, combining both filters remove cloud pixels that limit the ability to estimation the surface water contour.

As the cloud filtering causes potential gabs over the reservoir, shown in the left image of Figure 17, the contour of the area would have a lower amount region available for the construction of the water level distribution and the volume monitoring. Still, as the south side portrays, a part of the reservoir can be distinguished. Therefore, the example left image is combined with the right image within a 10-day window. Accepting a maximum error in the water level of 0.02 [m], computed from the available in-situ data series of the 88 selected reservoirs.

The right depiction of Figure 17 shows the resulting image of the temporal smoothing filter of the Ridgeway Reservoir. Here both images are mosaiced, combining the parts with clouds of the left images with the middle image.

Figure 17 Cloud filtering and reconstruction of the L&R that is affected by this noise

Snow noise removal

The snow/ice image removal was the following added noise remover applied in the suggested method for surface water contour determination was the snow/ice image removal. The limitation is caused by L&R that have the presents of snow and ice over the water surface. Therefore, limiting the ability of the NDWI/Otsu thresholding tool to build a water/land image successfully.

An example is given in Figure 18, showing the results of 2 images at different time intervals, December 2018 and June 2019. Here the land/water contour is given of lake Mayola (New Mexico, USA) in the top figures. At the same time, the respective water/land image is given in the bottom figures. Please note that the green in the bottom figures depicts the landmass and blue the water surface.

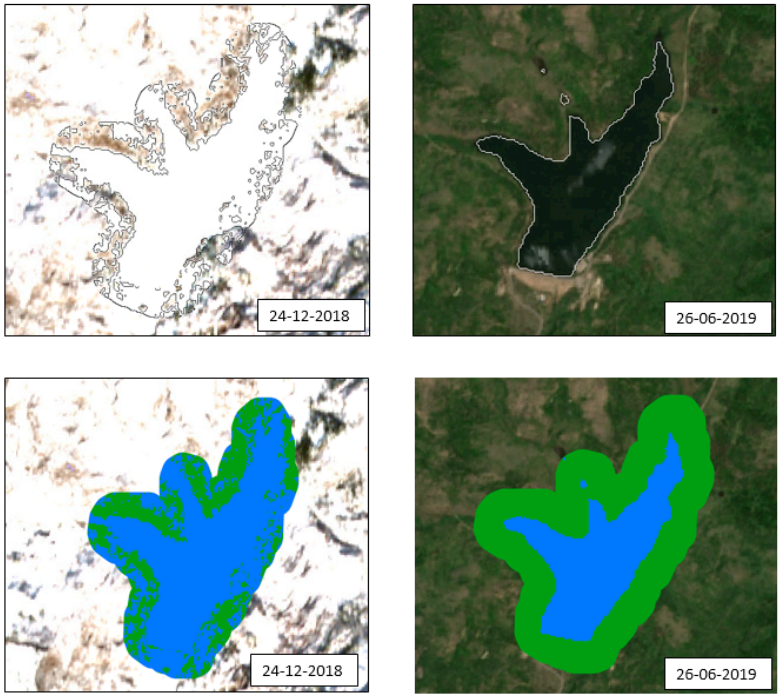

Figure 18 Effect of snow on the determination of the Surface contour of lake Mayola (Colorado, USA)

When comparing the winter images (left top/bottom) of lake Mayola, the snow in the region cannot correctly be distinguished from the land. Therefore, results in a water level that can be considerably higher than the original height and an incorrect volume for this lake.

As a result, this study considered two solutions for restricting the false water level elevations caused by the snow/ice noise. First, the JRC water-occurrence data was used to suppress false detections between land and water. Removing elevations from the distribution that are located in the areas larger than 0% and smaller than 80% water occurrence. Therefore, when the contour is falsely placed over a more significant elevation, the data will be removed from the water level distribution. Please note that none of the L&R selected by this study dried up during the case studies time window.

The second option is based on the study of Bonnema and Hossain (2017), which computed the fraction of usable Landsat images for each month. The study suggested that the usable images in the months December, January and February were relatively low. Therefore, the images from these three months were not considered and removed from the time series.

The resulting surface area is depicted in Figure 19, where the original time series is given in red, and the snow months removed in green.

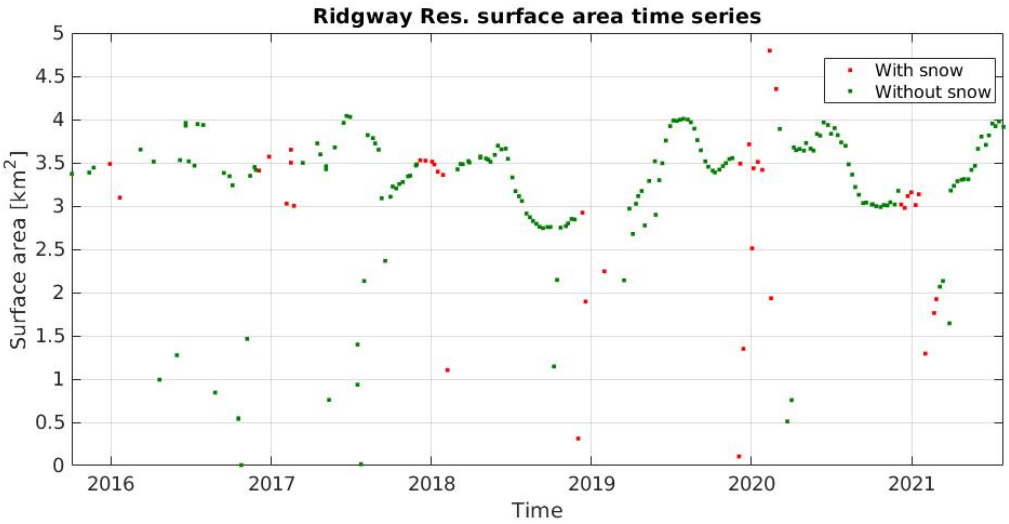

Figure 19 Surface area time series of the Ridgway reservoir, showing the images with the snow months (green) and without (red)

Note that the boundary created between the land and water classes, was computed with the canny edge detection method. Here the set threshold is kept at 0.99, while having a standard deviation of 0 was used (Donchyts et al., (2016)).

4.1.2 Water level extraction

The second part of the applied method, regarding the extraction of the water level the following steps were added or adjusted: the manner of how the water level is distribution is constructed, the noise removal filters and how the flattened pixels are classified in this study.

Creation of the water level distribution

The water level extraction for this study is explained with the following visualisation of Figure 20. Here the left depiction shows the artistic interpenetration of a minor part of the L&R, where 1 represents the water and 0 the land. The middle figure shows the small minor part of the border with the lower DEM elevation model.
The right figure depicts the resulting elevation distribution, extracted from the DEM, where the red line depicts the water level sampled with the mean.

Please note that the line created using the canny edge detection method is converted to an image therefore, each overlapping boundary pixel can collect the elevation. Applying a morphological operation to generate the pixel size of 2 [m].

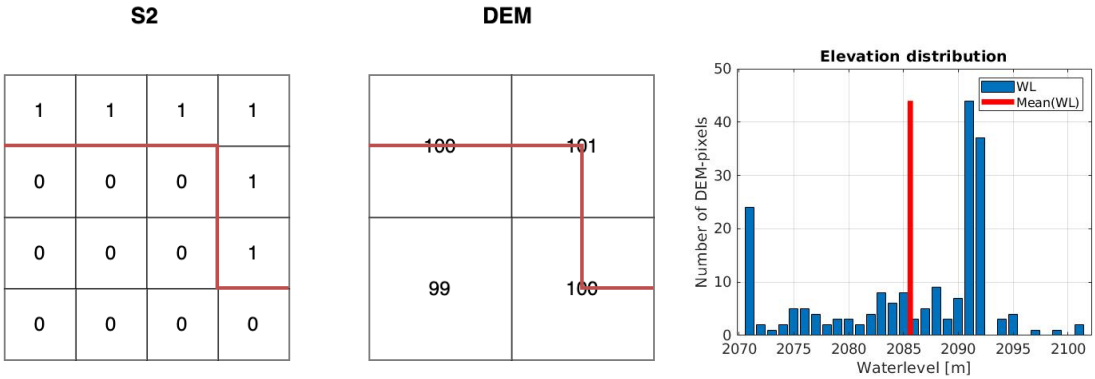

Figure 20 Method of elevation distribution creation for water level time series determination, showing the water/land border (left), the water level extraction (middle) and the resulting elevation distribution (right).

The mean sampling method will be applied to select the water level based on the distribution shown in the two cases. Since the average considers that, although the water level is taken constant, the spatial variability also influences the water level determination.

Two filters were considered to suppress noise that arises when using the elevation models to reduce potential false or elevations with a high vertical error from the distribution. First, since a water-occurrence filter is applied here, that considers that the surface area would not go to zero in the set period. Hence removing that the border pixels had made a false detection based on clouds or snow. The second filter is the gradient suppressor, which will be further discussed in the following subsection.

Slope analysis

To visualise the elevation error introduced by the gradient of the slope, the following visualisation is given in Figure 21. Showing two cross-profiles, including the change in water level over time (blue lines). The top reservoir portrays the effect of a relatively low gradient over distance, while the bottom example depicts the high gradient. The arrow drawn for each reservoir cross-profile portrays the elevation that can be measured whilst using this DEM.

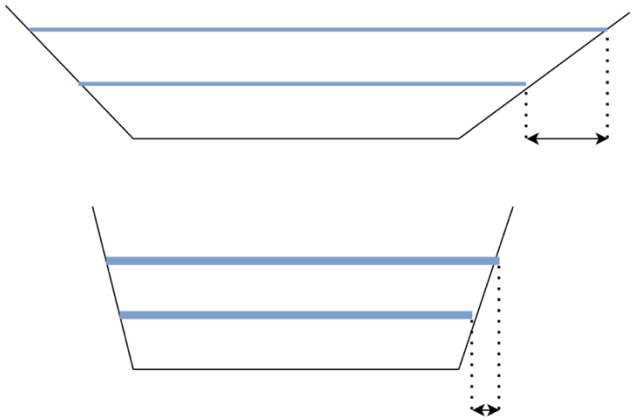

Figure 21 Water level extraction limitation by the slope of the L&R

When the spatial resolution of the DEM is larger than the portrayed arrow, no elevation variation will be found. Therefore, a constant water level is extracted from the pixels, while the depth increases, introducing the potential vertical error for the elevation and water level extraction.

For suppressing the errors caused by the slope of the L&R, the elevation having a higher gradient than 10% were removed from the water level distribution (Uuemaa et al., (2020), Fernandez et al., (2016)) The effect of the slope reduction filter, removing boundary elevations having a higher gradient than 10%, is given in Figure 22. Here the left images depict the original boundary, while the right shows the resulting border.

Figure 22 Effect of the slope and water occurrence noise reduction, for the construction of the water level distribution

Classification of flattened pixels

The classification of flat pixels present in water bodies of elevation models was key to extracting the correct water level and the implementation of the LBDEM tool. Therefore, two aspects were implemented for this study to support the classification process: the elevations gradient and water occurrence.

To visualise the first aspect, the elevations gradient, Figure 23 is given showing the Lemon (Colorado, USA) reservoir. Giving a representation of the elevations [m], where the left image shows the elevation levels and right the cross profile of the black line.

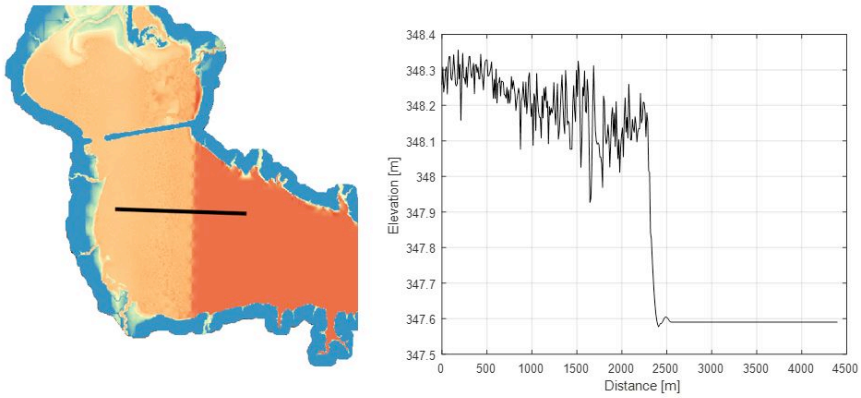

Figure 23 Visualization of the flat surface in the Lemon reservoir (Colorado, USA), where the black line represents the cross profile on the right

From Figure 23, it can be deducted that the flat elevations have a gradient of 0. Therefore, filtering based on this gradient will remove the reservoir parts where the bathymetry was not determined. The gradient classification method's limitation is that, for instance, beaches have the same gradient as the flat pixels. Since the height variation at these regions is relatively small, resulting in a zero gradient.

So, the second classification method introduced in this study is the water-occurrence of the water elevations as flat areas are present at regions where the water was present during the construction, therefore removing all the 0 gradient elevations that had a lower water occurrence than 70%.

Please consider that based on the proposed method for the classification of flat elevation, the following limitation was still present. The method neglects elevations that are present that are lower/depressed relative to the flat surface. The reason for this neglect is that the bathymetry is unknown for the available 88 L&R. Therefore, elevations that were potentially lower than the model could include the real waterbed. Nevertheless, this study considered the presence of depressed pixels to be neglectable small when analysing the results of 88 L&R.

The area was computed per elevation model containing flat elevations shown in Figure 25, portraying the effect per model of the 193 L&R smaller or equal to 5 km2. The “presence’ is computed by the total area found in the JRC water occurrence data divided by the area classified as flat.

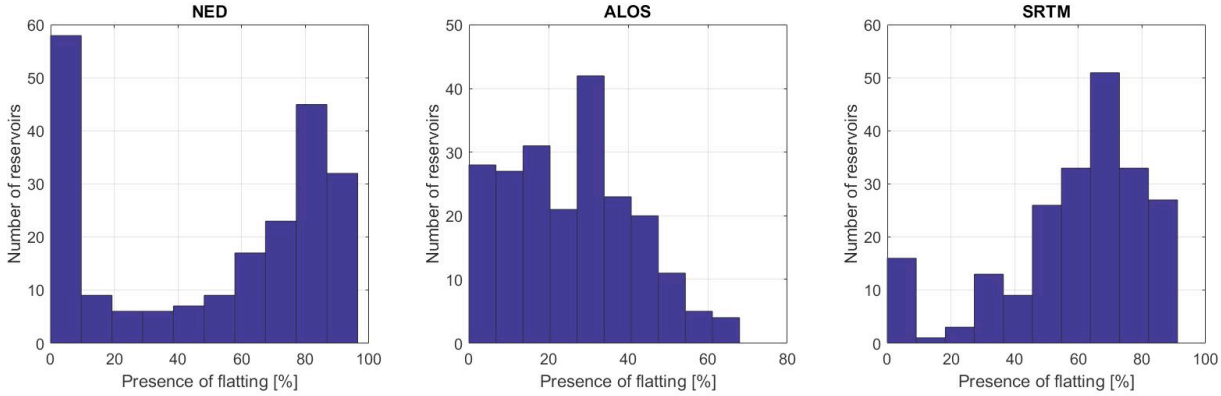

Figure 24 The presence of flatting in elevation models, based on all the small reservoirs in the USA, portraying the histograms of NED (left), ALOS (middle) and SRTM (right).

As the figure portrays, the NED model shows an interesting distribution. The L&R experiences either a small presence flatting or more than 60%. Likewise, the SRTM depicts the poorest results from the three models, where the distribution is centred at the 60 - 70% flatting for the 193 reservoirs. Finally, when looking at the ALOS model, the distribution shows that most reservoirs are experiencing less than 50% of the region.

Concluding that NED in most cases would have been the optimal selection choice based on the presence of flatting, whilst ALOS is depicting a relatively good distribution as an alternative. Nevertheless, the older SRTM would be the poorest choice for monitoring the reservoirs, based on the presence of flattened pixels without applying LBDEM.

4.1.3 Volume level estimation

For the last phase of the method, the depth capacity curves based on the DEM was added in comparison with the literature, while neglecting the results based on the volume models.

Depth capacity curves

With the extrapolated elevations and the extracted water-level time series, the depth capacity curves can be constructed. Like the USGS approach, these curves can be used to transform water levels to volume levels based on the selected reservoir. The minimum water level and the maximum water level of the extracted time were determined, constructing an input value to generate volumes based on the elevations of the selected DEM (with LBDEM).

An example of a depth-capacity curve is given in Figure 26. Showing the relationship between the water level and the volume [km3] for the Ridgway reservoir. Please note that for the LBDEM tool, a maximum depth threshold of 30m was utilised to linear extrapolate the elevations.

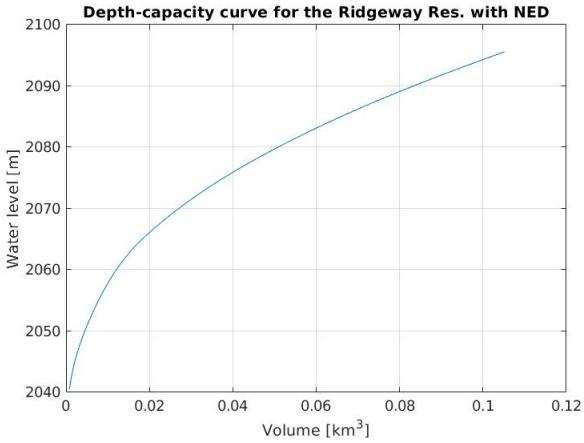

Figure 25 Depth Capacity curve, showing the relationship of the elevation against the volume of the reservoir, while using the LBDEM tool for extrapolating elevations.

The volume levels that are depicted here, show a rising trend for this reservoir. Meaning that when the water-level increases the volume increases.

Limitations of DEM volume estimation

The limitations that can arise when directly implementing a DEM with the flat elevation replaced, is the temporal resolution of the reservoirs in comparison with the construction of the models. Potentially leading to three situations, that can influence the volume time series estimation. Since for instance the satellite-mission flew prior to the construction of the reservoir or lake, therefore depicting a surface without the proper slopes and waterbed.

Also, a potentially limitation for using DEM is that the mission was not continues, (i.e., still updating the elevations on a regular basis). Therefore, leaving the possibility, that new features like a dam or artificial island are not included in the model. Thus, even when the correlation is high between the water-level and the surface area or the in-situ data, will result in a false absolute time series.

4.2 Data description

For this study three datasets are required for demonstrating the effect of the LBDEM tool.

- Multi-spectral imagery datasets, that are used for the classification of the water surface area of the reservoirs/lakes.
- Digital elevation models that essentially contain the elevations for the water-level estimation and the volume time series.
- In-situ data that has a higher vertical resolution than the DEM, which can be used to validate the estimated water-level and volume time series.

For the multi-spectral imagery dataset, the Sentinel-2 image collection will be used in the case study. This collection has a higher spatial resolution than the alternative free-accessible missions like Landsat-8 or MODIS. Also, the temporal resolution is relatively high, which is 5 days.

The elevation models selected for this study are the SRTM (RADAR), ALOS (Stereography) and the NED (combination). All three models are fully available for the L&R in the USA and represent different spatial resolutions, construction dates, and local and global models. The model that is considered for this study is referenced to the NAD83. Hence, a data conversion was applied to match the EGM96 geoid (like SRTM and ALOS). When looking at the spatial resolution of this model, the USGS supplies different types. This study utilises the 10m spatial resolution of the United States (CONUS).

Table 2 is presented with an overview of the available datasets. Here the spatial, vertical, and temporal resolutions are given, when the data was constructed or available, where the data was collected from and the source. For example, the vertical resolution of the elevation models differs per location; therefore, the minimum and maximum range are given. All the implemented datasets were collected from the Google Earth Catalogue.

Data	Spatial res. [m]	Vertical res. [m]	Temporal res.	Availability	Data source
Surface water contour					
Sentinel-2	10	-	5	2015 - now	European Union/ESA/Copernicus
JRC	30	-	-	1984 - 2021	EC JRC / Google
Water level extraction and volume variability determination					
SRTM	30	6 to 12	-	2000	NASA / USGS / JPL-Caltech
NED	10	2.44	-	2012	United States Geological Survey
ALOS	30	5 to 12	-	2006 to 2011	JAXA Earth Observation Research Center

Table 2 Summary of the used datasets for the case study

The USGS in-situ instruments

The in-situ data available for the validation of the extracted water level and volume data of the elevation models with LBDEM comprises two types. First, since the area of interest of this study focuses on the L&R located in the United States, the USGS database was considered for the water level and volume time series.

The USGS monitors the water level by use of numerous systems that be categorized by systems that are near a waterbody. These systems include the Basic float system, Bubble gages, Pressure transducers, Acoustic transducers, Acoustic transducers, RADAR stations, Optical (laser) stations, Rapid deployment Gages.

Each system has a vertical error in the magnitude of 0.01 ft (= mm order of magnitude) (Sauer and Turnipseed (2010)) while outputting data at a continuous interval. Please note that a designated office checked each time series before publishing the water level data. Therefore, ensuring the data has the set-vertical accuracy.

The resulting water level found by these instruments is then implemented to monitor the storage of the reservoir as the volume levels of the reservoirs are deducted by the depth-capacity curves, unique for each waterbody. The foundations are the bathymetric surveys or

the use of the water balance equation, where for the latter, the change in water-level the main volume level is. The curves are supplied to the USGS by the following sources:

- State Water Resources Control Board – Division of Water Rights Water Right License
- Natural Resources Conservation Service
- Department of Water Resources - Jurisdictional Dams

4.3 Case study set-up

The case study to determine the potential of the digital elevation models for estimating the volume variability of lakes and reservoirs will apply the water bodies of the area of interest. First, the water level extraction was validated to determine the accuracy levels of the method when the LBDEM was applied at the elevation models. Here the USGS in-situ data were considered for the validation of the DEM results. The validation comprises the relative water level series, where the correlation coefficient R^2 was used. While the absolute water level was validated by the root mean square error, the mean absolute error and standard deviation.

Please consider that the data where the LBDEM was not applied will be referenced to an "original". Likewise, when the lowest elevation in the L&R of the DEM was not lower than the maximum water level found in the In-situ data, the data was removed from the time series. To assess why the relative or absolute time series in some situations is not corresponding with the in-situ data, several L&R were selected to determine the limitations of the LBDEM tool for water level extraction.

Second, the model's volume variability was investigated using the selected 30 L&R, clarified in the area of interest. The same approach as the water level was used here, e.g., the relative (R^2) and absolute (RMSE) time series. Also, for the absolute time series, will each volume be compared to the in-situ data to see the immediate difference. The limitations found by the water level extraction with the in-situ data will be validated for the low volume correlated L&R.

5 Results

The results are presented into two parts, giving the impact of bathymetry extrapolation on the water level (§5.1). While the volume variability is analysed in the second part of the case study (§5.2).

5.1 Impact of bathymetry extrapolation on the water level estimation

When looking at the impact of LBDEM to estimation of the water level, the 88 selected L&R were analysed. Figure 27 shows two histograms that portray the correlation coefficient between the USGS in-situ data and the DEM water level. The left histogram represents the results without LBDEM. While the right shows the effect of LBDEM on the water level extraction. Please note that here the model was selected based on the highest correlation (R^2).

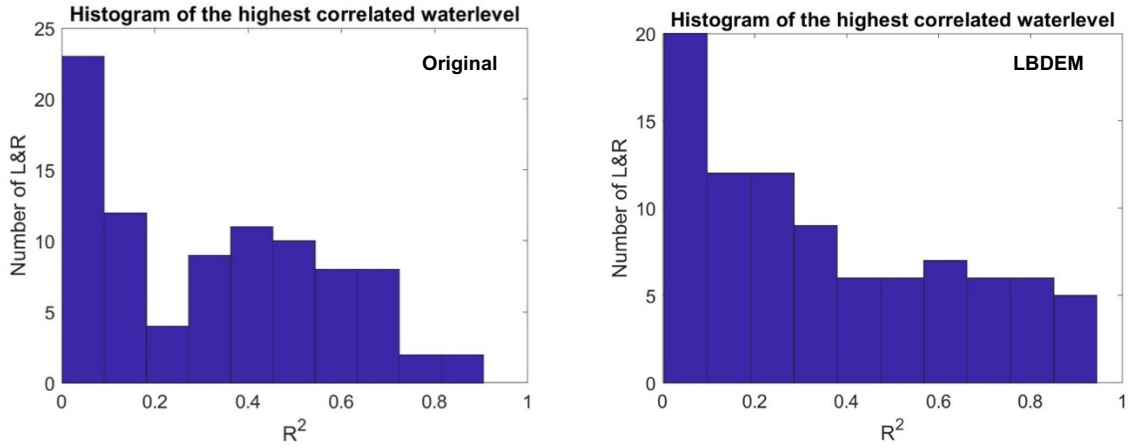

Figure 26 The water level correlation coefficient of the 88 L&R when the LBDEM is not applied (left) and when applied (right)

Striking is that the number of L&R that were able to extract the water level was increased when LBDEM was applied. Considering that the higher correlated L&R (R^2>0.6) rose from 13 to 22. Showing that when applying the tool, a general increasing effect can be noticed for the deduction of the relative water level time series based on the overall correlation coefficient.

The average RMSE, mode RMSE and the standard deviation of the three elevation models is presented in Table 3. The number of L&R is the number of waterbodies that corresponds with the mode of the RMSE. The results were achieved while using the LBDEM tool with a maximum depth threshold of 20 [m].

DEM	Avg. RMSE [m]	Mode RMSE [m]	Numb. of L&R	Standard deviation [m]
NED	4.2	1.3	44	4.6
ALOS	4.2	1.4	31	3.3
SRTM	4.4	3.7	31	3.7

Table 3 RMSE of the 88 L&R using the LBDEM tool

The results showed that the average RMSE remains constant with the ALOS and SRTM model when having a lower spatial model. Yet, the NED model has an advantage when looking at the mode of the RMSE, showing a water level error of 1.3 m. Interestingly the ALOS elevation model shows similar results, yet 10 L&R is lower than NED.

To investigate if the same pattern is seen between the elevation models for the relative time series, the 22 L&R that have a higher correlation than the 0.6, the following histograms are given in Figure 28. Portraying the results of each elevation, ALOS (left), SRTM (middle) and NED (right), depicting the correlation coefficient of the original DEM at the top and with LBDEM at the bottom.

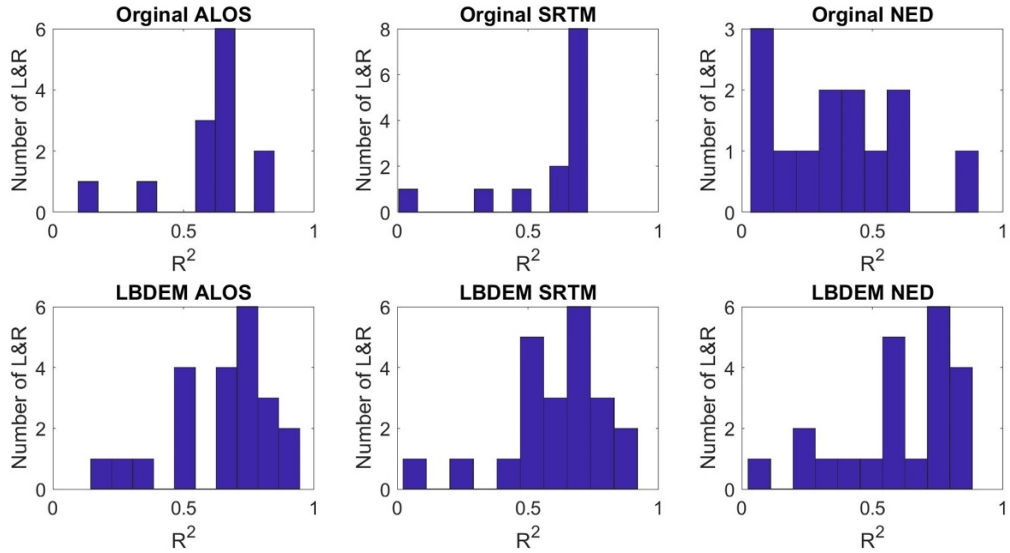

Figure 27 Histograms of the L&R where at least one model had a higher coefficient than 0.6 for the water level extraction

In general, the effect that can be seen that for more L&R the water level could be extracted when applying the LBDEM tool. The effect of LBDEM of the high correlated extracted water levels at the individual elevation models, the L&R where the available water level was monitored all have a high correlation. Implying that, in general, the spatial resolution did not directly affect the estimation of the relative water level.

The L&R with a R^2 higher than 0.8 after the LBDEM tool was applied is portrayed in Figure 29. Demonstrating the models of the L&R, where the water level time series showed a distinct change. Here the in-situ data is shown in yellow, the LBDEM data in red and the original data in blue.

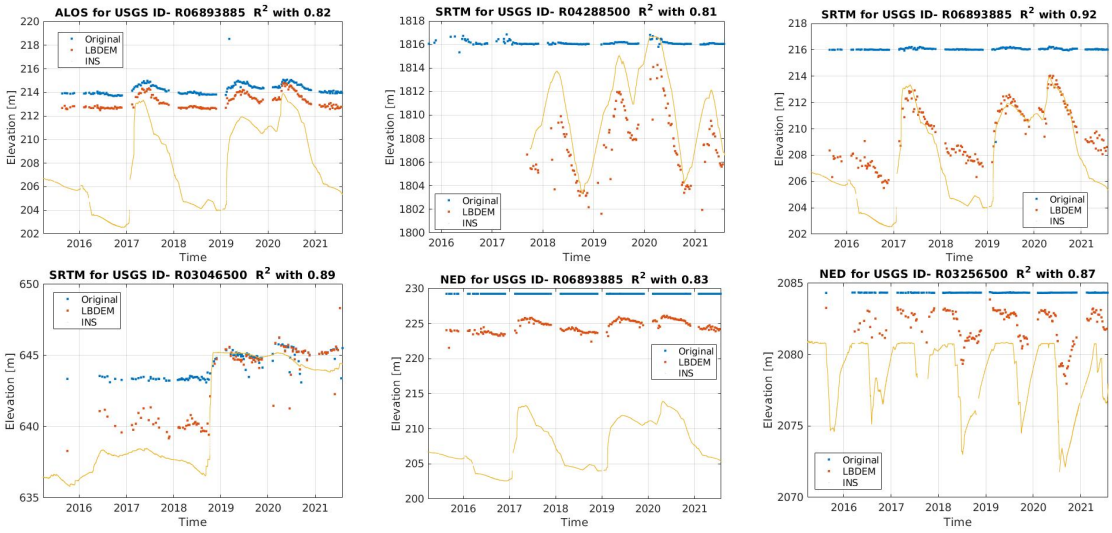

Figure 28 Water level time series of the L&R with a correlation coefficient of 0.8 was found in the LBDEM time series. Each plot sows the USGS in-situ data (yellow), the original (blue) and LBDEM (red) affected timeseries

The first feature that can be noticed is the variation in the water level. When looking at the water level variation at the L&R with a low correlation, the results typically showed an in-situ variation of the 1 [m]. The results of Figure 29, portrayed a variation is observed to be typical 10 [m], while in Appendix B, the water level variation should have at least a 10 [m] variation. To visualise the effect of between the low and high correlated elevation variation, the relationship between the results of applying the LBDEM and the in-situ data is given in Figure 30.

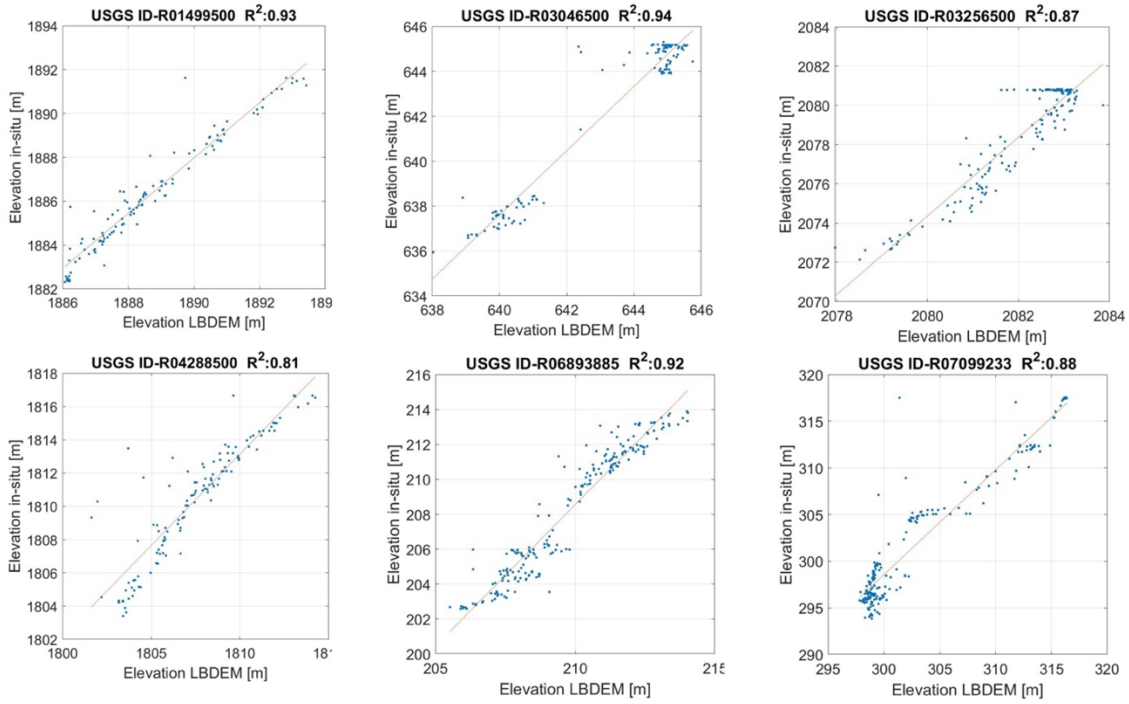

Figure 29 Visualization of the relationship between the LBDEM and in-situ data, fort he L&R that had a larger correlation coefficient than 0.8.

Secondly the region at which the LBDEM tool could be applied, influences the water level extraction relative to the in-situ data. The amount of region that is available for the estimation of the water level increases, based on the slope noise reductor. To visualise the applicable surface, the small Nichols reservoir is given, where both the original (Figure 31) and LBDEM (Figure 32) is depict with the three elevation models (ALOS, NED and SRTM).

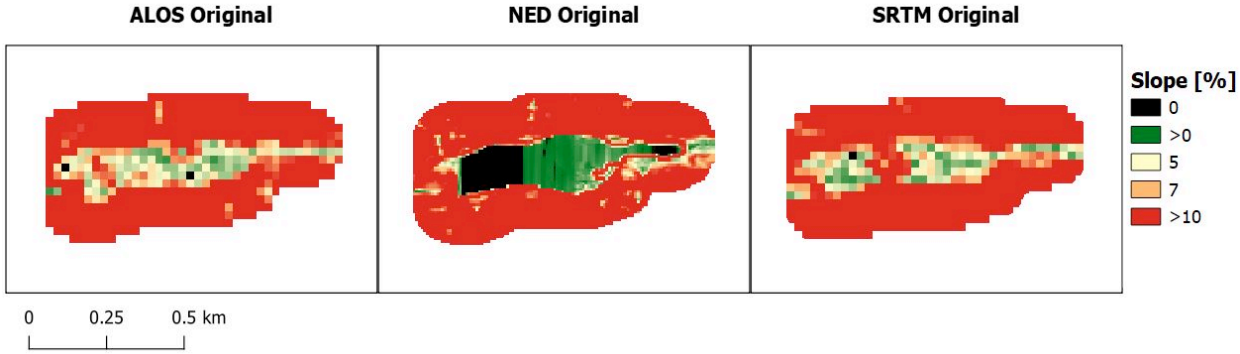

Figure 30 Slopes of the Nichols reservoir for ALOS (left), NED (middle) and the SRTM (right), where the LBDEM was not implemented

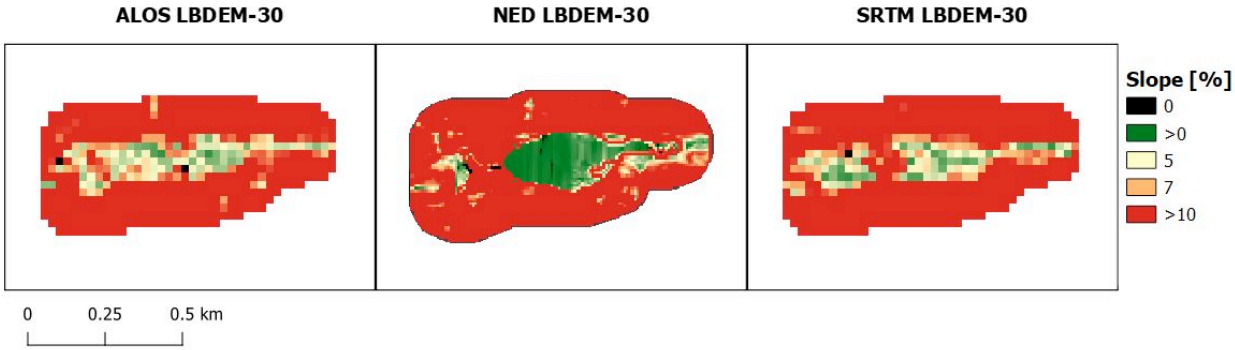

Figure 31 Slopes of the Nichols reservoir for ALOS (left), NED (middle) and the SRTM (right), where the LBDEM was implemented

Striking is that ALOS and SRTM have a coarse representation of the reservoir due to the low spatial resolution (30 [m]). The Nichols reservoir is not larger than 0.15 $km^{2,}$ this in combination with the large spatial resolution, results in that only a minor part of the waterbed was found in the ALOS and SRTM model. Resulting that the elevation models were the LBDEM tool was implemented for the Nichols reservoir did not have any effect on the extraction of the water levels.

The NED representation depicts a larger green region in Figure 31 that can be effectively used for the LBDEM tool to extrapolate the elevations. However, due to the region's small size and that boundary has a slope with a high gradient. Caused the two kernels of LBDEM to consider more significant elevation differences for the extrapolation part. Thus, there was no increase in region for estimating the water level when the surface area declined into the flat-pixel area.

The opposite effect is seen at a relative larger L&R, where sufficient water level variation was seen. In Figure 33 and 34 is the El Captain reservoir given, for the ALOS (left), NED (middle) and SRTM (right).

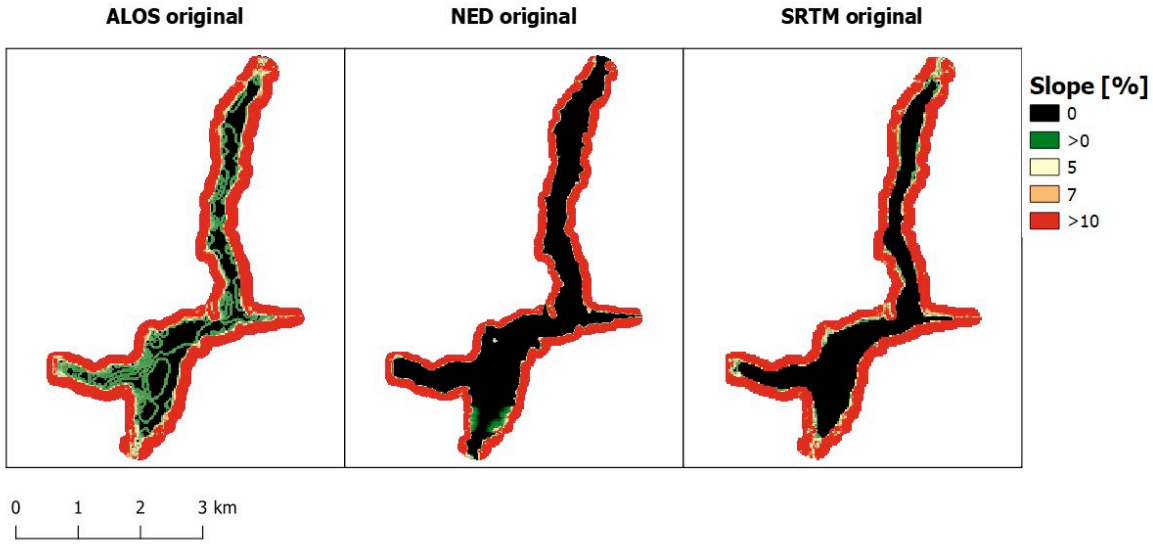

Figure 32 Slopes of the El Capitain reservoir for ALOS (left), NED (middle) and the SRTM (right), were the LBDEM was not implemented

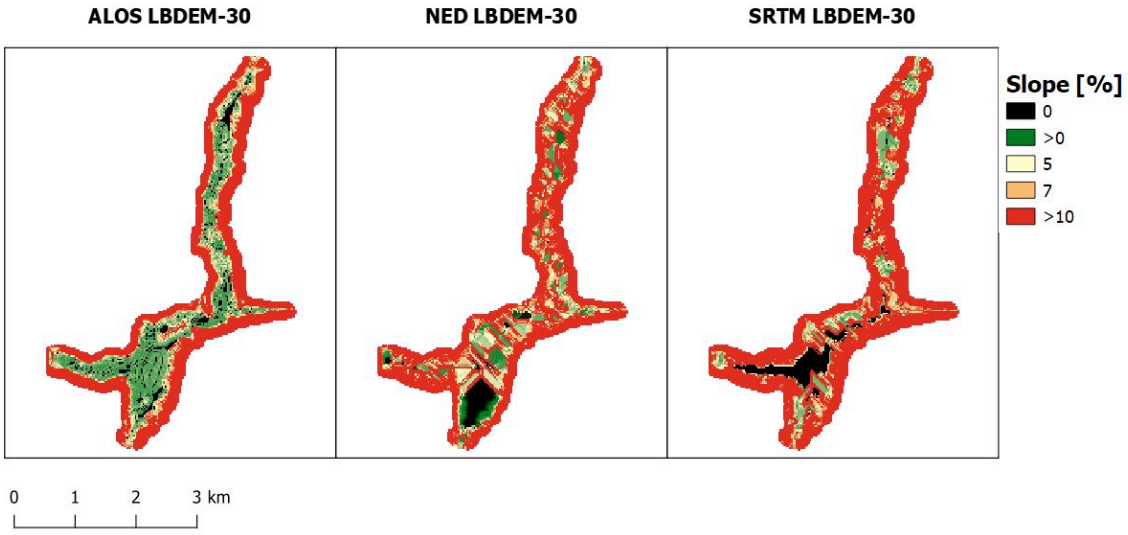

Figure 33 Slopes of the Nichols reservoir for ALOS (left), NED (middle) and the SRTM (right), were the LBDEM was implemented

The effect for the el Captain reservoir is visible for all three elevation models. As the boundary region for this reservoir has a low gradient at the boundary, therefore the extrapolated elevations can be utilised for the determination of the water level. Resulting in an increased region for water level determination when the surface water declines.

Also, the flat surface is for each model extrapolated when using the LBDEM-30m threshold. Showing that when using the LBDEM, potentially not all the flat surfaces will be replaced with the new elevations. Concluding that when the bathymetry of the L&R is unknown, the correct maximum depth threshold will not be found. Therefore, when taking the limitation into inconsideration, it is favourable to use the tool for extracting relative water levels.

Effects of using higher spatial resolution imagery data

For demonstrating the effects of higher spatial resolution for estimating surface area and the resulting water level, the 88 reservoirs are validated for both the Landsat-8 and Sentinel-2. Table 4 provides the mean absolute error [m], the standard deviation [m] and RMSE [m] compared to the USGS in-situ data for both multi-spectral instruments that were used to estimate the water level. Please note that for this validation, the highest correlation was chosen for representing the optimal elevation model.

Optical	Mean absolute error [m]	RMSE [m]	Standard deviation [m]
S2	3.53	4.92	4.27
L8	3.91	5.63	4.98

Table 4 Results of the comparison between MAE, RMSE, SD of constructed water contours based on the time series by S2 and L8.

The mean absolute difference between the two optical determinations is relatively small being 0.38 [m], while the RMSE had a variation of 0.71 [m]. Showing that, on average the selection of a lower spatial Landsat-8 multi-spectral data does not have a direct influence on the vertical error in the water level determination.

Figure 35 visualises the water surface [km2] through time for the Lemon reservoir and Nichols reservoir. When analysing the effect of the temporal differences between the two datasets, the following feature was noticed: the L8 data had a relatively higher noise level than the S2 data.

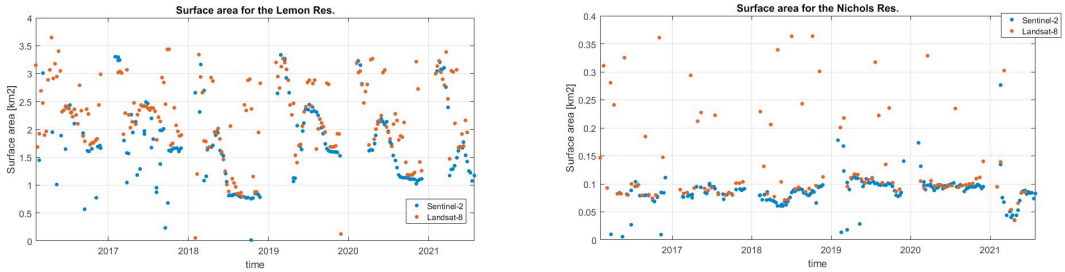

Figure 34 Surface area time series for the Lemon and Nichols reservoirs, were the results of Sentinel-2 (blue) and Landsat-8 (red) are given

Secondly, both depictions show that L8 had a lower number of images available than S2 for creating the binary images between land and water. When taking the complete distribution of L&R, the number of images containing WL data from 2016 (without the winter months) for L8 was 13488 images, while S2 14387 images were available.

Thus, showing that for a 6-year time window S2 had 899 images with a lower noise level. Therefore, the beneficial effect of using the S2 in comparison to frequent used L8, would result showed to have more usable images while having less effect of the anomalies discussed in Chapter 4.

Effects of selecting the optimal model

For demonstrating that the proposed selection method operates for the 88 reservoirs, the following comparison was conducted. Based on the correlation between the in-situ data and the water level, the optimal elevation model should have the highest R2. Hence the least flat pixels selection method was validated against the model with the highest correlation. Accordingly, the results are given in Table 5, showing the number of reservoirs where the correct model was selected.

Method	False selected	Correct selected	Optimal DEM
ALOS	38	32	40
NED	11	4	30
SRTM	3	0	18
Least flattened	52	36	-

Table 5 Results of the comparison of selecting the optimal elevation model based on the highest correlation coefficient between the DEM and USGS in-situ WL-data, here showing the number of L&R that selected the model falsely and correct

Table 5 shows, using the least flattened surface method resulted in elevation models that did not have the highest correlation with the in-situ data. The reason behind this higher amount of false, selected reservoirs is that the ALOS elevation model (as shown in does include as much flattened the water-pixels in the reservoir based on the gradient. The pixels at higher water occurrence are not altered, like NED or SRTM. Therefore, this DEM would usually be selected more frequently than SRTM or NED. So, a lower amount of the correctly selected elevation models to be selected to estimate the volume time series with LBDEM.

5.2 Impact of elevation extrapolation on the volume level estimation

The absolute volume time series

The USGS monitors a smaller distribution of L&R for the volume level; the 30 pre-selected waterbodies of the area of interest were analysed. The difference in volume level per time interval of the L&R was computed, giving an error between the LBDEM and the USGS in-situ data. The results are depicted in Figure 36, demonstrating the effect of applying the LBDEM tool at different maximum depth thresholds. Here, LBDEM-0 represents the original data, while the -10, -20 and -30 are the respective maximum depth thresholds.

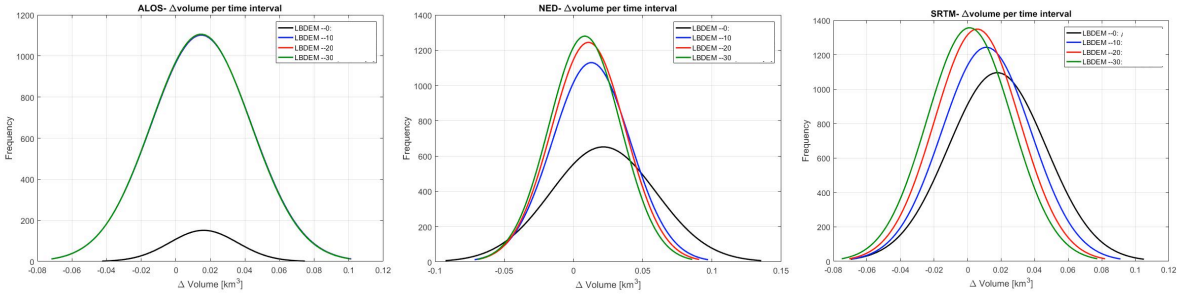

Figure 35 Comparison between the USGS in-situ volume data and ALOS (left), NED (middle) and SRTM (right) data, were LBDEM-0 resents the unaffected data, while -10, -20 and -30 shows the maximum depth threshold.

The distributions in Figure 36 showed two striking features. The first feature is that the distribution of volumes increases. Thus, implying that the LBDEM tool for volume variability monitoring increased the amount available to the L&R.
The next feature is improvements seen in the mode of each distribution, where SRTM even show that the distribution is centred at a 0 km3 difference with the in-situ data.

Figure 36 also showed the average RMSE between the in-situ and the DEM data. In line with the study of Vanthof and Kelly. (2019) study, the RMSE is computed as a ratio of the maximum volume level found by the monitoring stations. In Table 6, the results are given for each elevation model without and with LBDEM at a 20 [m] maximum depth threshold.

DEM-Name	Without LBDEM	With LBDEM-20 [m]
NED	11.8%	5.4%
ALOS	2.3%	2.0%
SRTM	5.7%	0.8%

Table 6 RMSE relative to the maximum amount of in-situ volume level found for NED, ALOS and SRTM.

Table 6 showed that the RMSE of the volume level decreased when the tool was applied. Thus, even for relatively older models (i.e., STRM), while correctly classifying the flat pixels, the model can improve the absolute time series of the L&R. The increase in both absolute volume levels and the RMSE was visualised in Figure 36. The volume time series of SRTM is given for the Ridgeway res., Fruit Growers res., lake Elanor and the Lemon Reservoir. The original volume is depicted in the top figures and the LBDEM in the bottom.

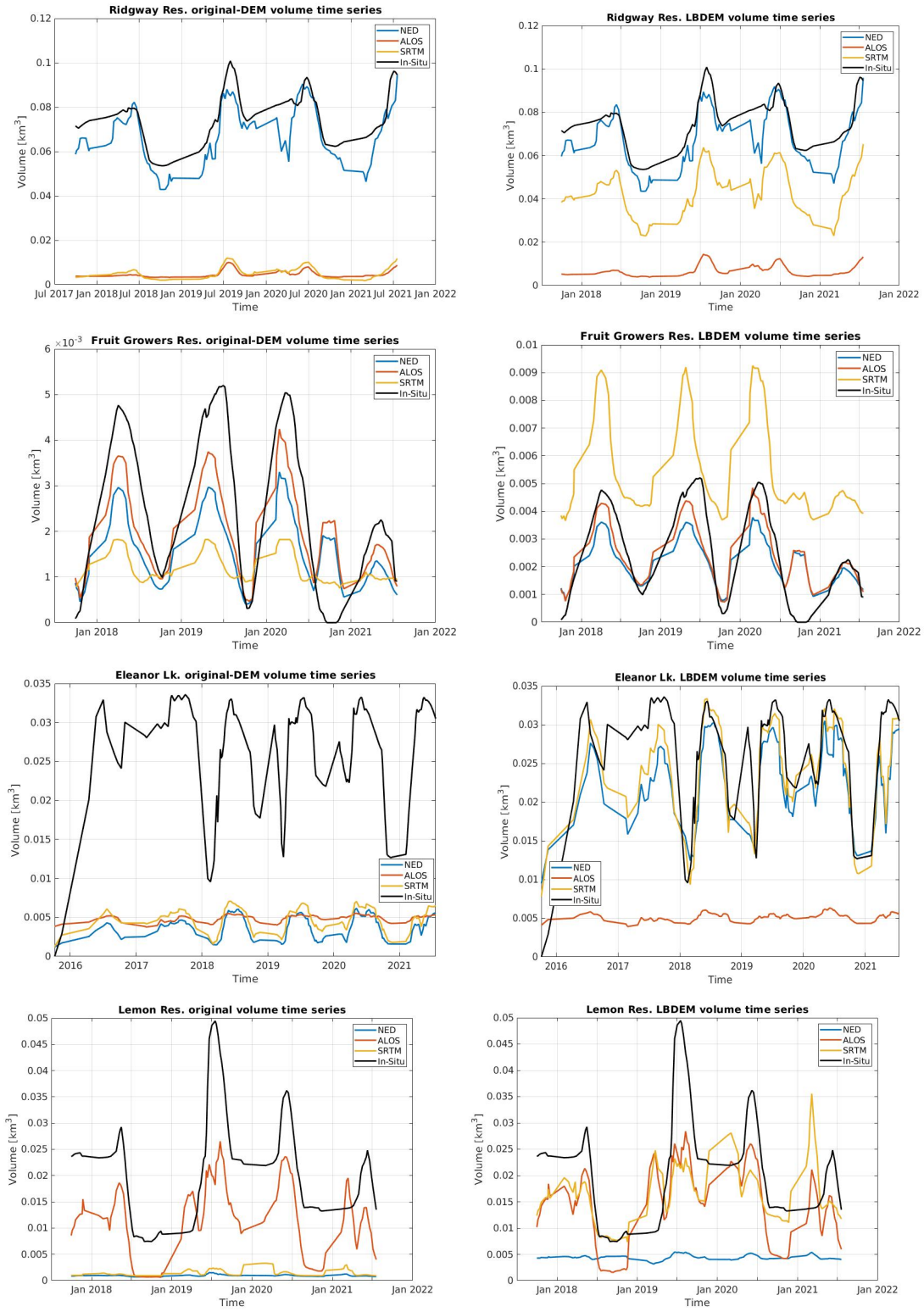

Figure 36 Volume time series of the three DEM, for the Ridgeway reservoir, Fruit Growers reservoir, lake Eleanor and Lemon reservoir, where the left shows the original data and the right the LBDEM results

The time series shows that when implementing the LBDEM tool, more regions become available to monitor the L&R. Therefore, decreasing the difference between both the in-situ data and the found DEM data.

The relative volume time series

The relative volume series was assessed using the correlation coefficient between the LBDEM implement and the in-situ time series. The selected 30 L&R are visualised in the following six histograms of Figure 38. The original and the tool implemented correlation is portrayed to demonstrate the effect of both the spatial and LBDEM.

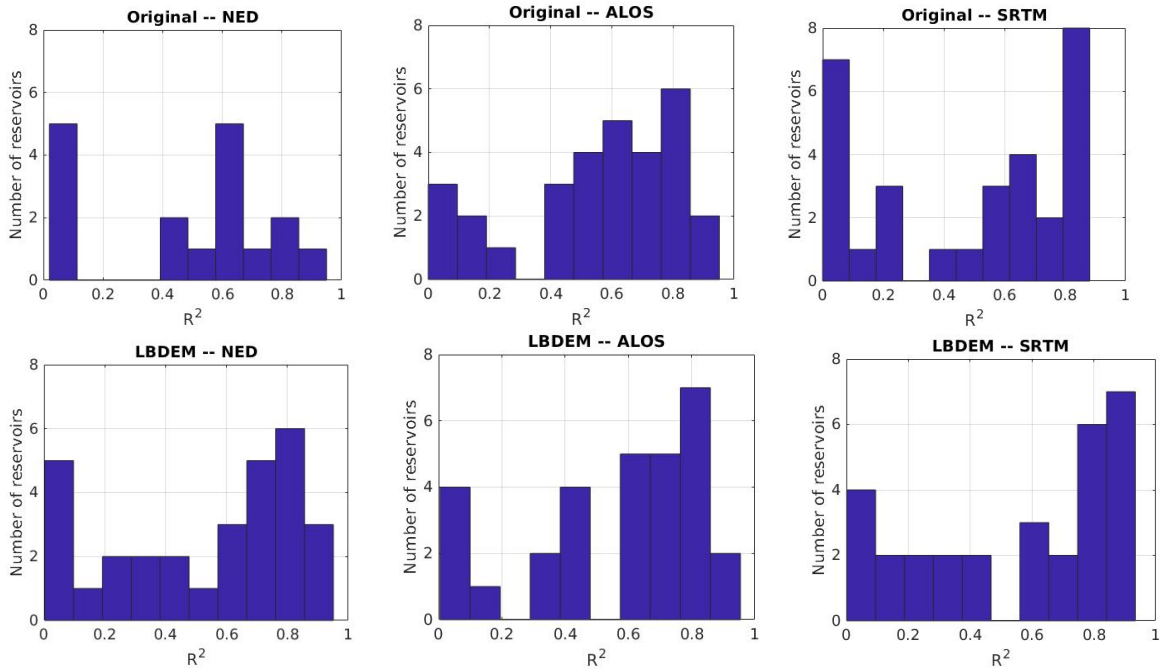

Figure 37 The correlation coefficient for each model, where the USGS volume is compared against the DEM without (top) and with LBDEM (bottom).

The first striking feature that can be deducted from the histograms was the number of high correlated L&R increases when applying the LBDEM tool. In line with the results seen of the water level, showing more L&R were able to be implemented to estimate the volume.
The second feature was applying the three different elevation models, depicting a minor effect in the correlation coefficient. ALOS had the highest number of L&R with an R2 higher than 0.6, while also being the model with the least region altered by the LBDEM tool.

The results showed that an increase in monitored L&R can be distinguished for the models containing the highest flatting (NED and SRTM). At the same time, the number of L&R that was able to monitor the volume remained constant for each elevation model, including a relatively high correlation coefficient.

Limitations to the LBDEM volume estimation

Table 7 supplies the following characteristics of the seven lakes and reservoirs that had a low correlation coefficient (<0.3), which help to deduct the limitations found by analysing the results of the water level (i.e., low water level variation and high gradient). Therefore, showing the average surface area, average water level variation, the correlation coefficient of the water level compared to the in-situ data and the amount of region of the DEM having a lower gradient than 10%. For comparison, the NED elevation model of the Ridgeway reservoir is given, including the bathymetry.

						Region [%]	
Name	Model	R^2 - Vol.	Avg. SA [km^2]	Avg. dWL [m]	R2 – WL	Flat	Gradient (<10)
Monroe City	ALOS	0.07	0.30	0.01	0.62	88	54
Mayola	NED	0.26	0.44	3.9e-4	0.43	27	38
Silver Jack	ALOS	0.51	0.96	0.09	0.16	40	54
Vail	SRTM	0.55	1.6	0.01	0.56	29	60
Donnel	ALOS	0.35	1.65	0.12	0.15	33	27
Tulloch	ALOS	0.33	3.52	0.0039	0.06	27	56
Ridgeway	NED	0.80	3.18	0.017	0.91	0	58
Alisal	ALOS	0.86	0.28	12.9 e-4	0.68	34	41

Table 7 Results of the low correlation volume L&R, where the type, average surface area, average difference in water level and the correlation in water level is given.

Compared with the L&R with a high correlation, the average difference is within the meter magnitude and has a relatively high-water level correlation. However, the size of the L&R had a minor influence on the determination, as, for instance, the Alisal reservoir, which had a low water level correlation, has a 0.86 volume correlation coefficient.

Since the results are based on constructing a depth-capacity curve, which was in line with the method of the USGS, the water level governs the construction of the volume time series. For instance, for the Monroe City Lake, the water level varies on average 0.1 [m] over time, leading to a lower likelihood for estimating the volume time series. In comparison, the water level of for instance the el captain reservoir (Appendix-B) showed a water level variation of more than 10 [m], therefore having sufficient vertical differences which can be used to estimate the water level and, therefore, the volume levels.

Based on the volume results, the following limitations hindered the volume monitoring with LBDEM; (1) the variability of the surface and water level over time, and (2) the increase in the region at which the water level (and the volume) could be determined.

6 Discussion

6.1 Water level estimation by use of the digital elevation models

6.1.1 General results

The results found in the first part of the case study, that is the water level was determined with an average RMSE of 4.2 to 4.4 [m] and a mode of 1.27 to 3.27 [m] for the model with the highest correlation between the USGS in-situ data and the water level, correspond to the results of Vanthof and Kelly. (2019), Deng et al., (2020), Zhang et al., (2014), and Weekley and Li (2021).

The literature results are based on using advanced smoothing algorithms, like a moving average polynomial (Avissee et al., (2017)) or pre-noise suppression (Weekley and Li (2021)) for the input values. The results of this work, however, were constructed without these smoothing algorithms other than snow and cloud smoothing. The latter clearly demonstrates the advance of the noise reduction.

The comparison between the different elevation models showed little difference between the correlation or RMSE; however, the number of L&R that had a low RMSE was higher for the NED and ALOS models. Hence, indicating that relatively newer constructed elevation models have an increased probability of extracting the water levels. However, the classification based on the gradient prohibited the ALOS model from fully implementing the LBDEM tool. Therefore, the results are more in the advantage of the NED model, were ALOS could be severe as a back-up DEM.

The current method neglects the influence of vegetation along the boundary of the reservoir. If trees are present, the processing pipeline does not remove these elevations from the distribution. Taken into consideration that NED is a bare earth model, while ALOS and SRTM are surface models. Introducing an error in the water level could have potentially limited the effect of the LBDEM, as higher gradients were experienced by the ALOS and SRTM model.

A closer look at the results revealed that a limited amount L&R showed a lower correlation between water level extract from the DEMs and the USGS in-situ data when using the LBDEM tool. Consequently, the current DEM had limited validity of the extraction water level elevations of these L&R. Cleary indicating the limitations of the LBDEM tool and method. These limitations were linked to the number of region available for the extraction of the water level and the small variation in the time series. Hence little effect of implementing further noise suppressing filters of contour pixels between land/water is expected.

The main source of error in this work is connected to the lack of the lowest depth knowledge of the L&R. The maximum depth threshold, used in the LBDEM tool, caused an error with an unknown magnitude. A solution to is given by Zhang et al., (2014), who used a labour-intensive method to establish the lowest depth in absolute terms. The method presented in this work should in a relative manner regarding the water level extraction.

6.1.2 Water level extraction with different multi-spectral imagery

The effect of applying Sentinel-2 and Landsat-8 multi-spectral imagery data proved a minor increase in the average water level error compared to the in-situ data. Concluding surface area contours were similar, therefore it subtracted similar water level distributions.

The temporal resolution of applying the S2 compared to L8 showed a positive effect on the surface area time series. Since the S2 has a higher temporal resolution, multiple images can be implemented within the set period for the cloud smoothing filters. While L8 only generally had one image, therefore having potential gaps in the data that was not filed by additional images. Confirming the suggestion made by the study of Deng et al., (2020), that Sentinel-2 image would be beneficial for the extraction of water levels.

The limitation that was not considered by results of this work is that S2 has a smaller time span than L8, Since the mission only started supplying images for the USA between 2015 and 2017. Creating a potentially small window to compare both multi-spectral analysis image collections of the surface water extent. Furthermore, it should be taken into consideration the winter months generally have a low number of usable images (Bonnema and Hossain., 2017) therefore decreasing the number of available images for L8.

6.1.3 Water level extraction by the optimal elevation model

The Weekley and Li (2021) study suggests selecting the optimal elevation model for global implementation based on the least number of flat elevations. Results of the case study demonstrated that the suggested method would lead to 52 falsely selected L& and an over selection of the ALOS model. As this model compared to the NED and SRTM replaced the bathymetry less often with zero-gradient elevations.

Still, it was beyond the scope of the study to develop a new selection method for the noise levels found in the ALOS elevation model as the purpose was only to provide insight if the method could be implemented on a global scale. Therefore, the results can be considered applicable for answering the research question.

6.2 The implementation of LBDEM for assessment of the volume variability

The results demonstrated an increase in correlation between the volume variability of the USGS in-situ data and the LBDEM implemented elevation model time series. Therefore, suggesting the DEM can be implemented to assess L&R in the USA since most of the L&R had a higher correlation (>0.6) than the original elevation model. Therefore, supporting the hypothesis that the linear extrapolation of the elevation data positively affects the volume time series created by the depth-capacity curves. Interestingly, confirmers the claims of Liebe (2005), that the pyramid shape and power-law equation are applicable for the volume variability.

The results contradict the claims made by the Vanthof and Kelly., (2019) study on volume estimation, since the results of this thesis estimated a lower RMSE ratio to the maximum in-situ data. For instance, the SRTM model had a volume RMSE of 0.8% compared to the maximum USGS in-situ data.

A closer look at the results between the three elevations, suggested that the implementation of the spatial resolutions did not directly affect the assessment of the volume variability. This because the NED had similar results to ALOS or SRTM for the correlation coefficient and RMSE. The respective results between the elevation models did support the hypothesis, that models with higher spatial resolutions should have a sharper shape of the L&R. Still the reliability of the results is impacted by the fact that only the USA is considered, which is therefore a constrained in this work. The global implementation is to be validated in future work.

In comparison with the literature, the results demonstrated that volume variation could be found with DEM when the LBDEM tool is applied, accepting the found limitations. Furthermore, the results build on the suggestions made by or instance, Deng et al., (2020), Vanthof and Kelly (2019), as the studies showed that volume could be determined by self-made elevation models based on TanDEM-X.

An interesting conclusion taken from the results is that the different L&R responded differently to the LBDEM tool, since the maximum depth threshold could go deeper than the actual bathymetry. This influenced the differences with the in-situ data. The latter implies that hydrographic surveys will still be needed to assess the real maximum depth threshold. In line with the Pan et al., (2019)) study, that shows the relative in-and-out flow is achievable when applying MDEM, the LBDEM tool was without sufficient knowledge to estimate the relative volume variability.

7 Conclusions

To assess the usability of high-resolution digital elevation models for extracting water levels and to compute the variability of the volume of lakes and reservoirs, the Linear Bathymetry for Digital Elevation models was developed. This was successfully demonstrated in the case study since the overall difference between the volume and the in-situ time series decreased from 11.9% for NED to 5.4%, for ALOS from 2.3% to 2.0%, and for SRTM from 5.0% to 0.8%.

The second and third objectives, providing an insight into the effect of applying elevation models for the estimation of the volume variability and monitoring of smaller L&R, were successfully found by the case study performed in the USA. LBDEM was implemented at the area of interest, containing 88 L&R in the USA to extract the water level. From this set, 30 L&R were selected for validation of the volume variability, as it contained volume in-situ data.

The results of this case study provided an insight into the effects that the extrapolated elevations have on the ability to monitor L&R. The NED, ALOS, and SRTM digital elevation models were validated against the USGS in-situ data. Therefore, providing an answer to the formulated sub-questions of Chapter 1.

What is the effect of using higher resolution imagery data for the determination of the water level?

The results showed that, when based on the spatial resolution, a minimum variation was seen between Landsat-8 (pixel size of 30 [m]) and Sentinel-2 (10 [m] pixel size). The 88 reservoirs demonstrated that S2 had a 0.71m lower RMSE than L8, which is neglectable considering the vertical accuracy of the different elevation models. The beneficial effect was noticed when analysing the higher temporal resolution of S2. Since 889 more images can be used over a time span of 6-years while having a lower noise level in the surface area time series. Considering this result, the hypothesis that higher resolution spectral imagery has a beneficial effect on the extraction of water elevations was confirmed.

What are the benefits of using higher resolution elevation models to determine the variability in the water level and volume?

The comparison between the different spatial resolution DEMs regarding the water level showed two features. Firstly, the average RMSE did not vary for the 88 L&R between the three elevation models. Secondly, when taking the mode of the RMSE, the NED and ALOS it showed an improvement to an error of 1.27 [m], respectively for 40 and 30 L&R. Implying that the spatial resolution did not influence the water level determination at the moment of construction. Since more recent models have a higher lower vertical error compared to the older SRTM model. The same phenomenon was demonstrated for the variability in the volume of the 30 L&R. No significant difference between the three DEMs observed for the correlation coefficient and RMSE after applying the LBDEM model.

What are the benefits of using the least flattened DEM to improve the estimation of volume variations?

For the 88 available L&R, the optimal DEM selection method, based on the least flat elevation, showed that ALOS model was 38 time over-selected while at the same a higher noise ratio at the waterbed. Also, 43% of the distribution had an optimal DEM that did not contain the highest correlation coefficient of the three elevation models. Therefore concluding, that the selection method based on the least-flat elevation would not result in the optimal DEM.

What are the effects of extrapolating elevations for estimating the volume time series?

The first significant effect observed, when extrapolating the elevations, was that more L&R could be monitored. The RMSE reduced for the 30 selected cases, especially for the SRTM model, showing a 0.8% RMSE. The volume variability can be determined with the LBDEM tool.

The second effect was that the absolute difference between the volume time series reduced for the different LBDEM maximum depth thresholds, implying that the tool creates more regions that can be utilized in order to assess the volume variation.

The exceptions demonstrated that the main limitations of using the LBDEM tool were the high slope values at the border regions between land and water, the spatial scale not detecting the flat elevations in small L&R, and the actual depth of the bathymetry is unknown. Therefore, although the RMSE reduced for each model, the relative volume variability would be more favourable when a sufficient region is available to extract the water level.

Thus, considering these conclusions, the following answer to the main research question can be formulate:

What is the potential of applying elevation models to monitor the volume variability of lakes and reservoirs, when replacing the flat elevations with extrapolated depths?

When using the Sentinel-2 data to construct surface areas, a smoother time series can be achieved and thus creating higher accurate water/land borders. Therefore, showing that the water level is estimated within the vertical errors of the model. The suggested least flattened selection procedure did not yield any beneficial results for the monitoring procedure. The results showed an over selection and choosing in-correct DEM for the water extraction. Nonetheless, the results demonstrated the potential for the global models to monitor the volume variability of smaller reservoirs without external altimetry data. The LBDEM tool suggested those elevations could be extrapolated, fitting a more realistic shape of the reservoir at areas where the bathymetry was flattened or not found. In conclusion, volume variability of lakes and reservoirs can be monitored with LBDEM, within the presented limitations.

Accurate information for extracting the water level and assessing the volume variability of lakes and reservoirs currently depends on extensive hydrographic surveys. This work provides guidelines for an alternative method: the Linear Bathymetry for Digital Elevation Models tool

8 Recommendations

This work successfully presented the first version of LBDEM for extrapolating elevations at classified flat regions. Nevertheless, LBDEM is still limited by several parts of the tool. Since the minimum threshold could potentially be automated when combined with, for instance, ICESat-2 or other altimetry data.

Another improvement for LBDEM is that the flattened surface is lowered based on the gradient between the elevations. However, as the study of Pan et al., (2019) demonstrated, the MDEM algorithm uses the flood patterns to simulate bathymetry. Hence a fusion of both methods could benefit from applying elevation models for monitoring the volume levels.
Likewise, the tool could be improved in the simulated depths, which is currently conducted by a linear interpolation method. Hence, other methods and shapes could be explored to determine which interpolation technique would best simulate depths according to the elevation gradient at the reservoirs/lake's boundary.

Considering that this study focuses on models with relatively higher spatial resolutions, future studies could analyse the effect of applying, for instance, the WorldDEM or NED3. Both have considerably higher spatial resolutions, therefore creating more acceptable input data for LBDEM. In the same manner, the input of higher resolution elevation models can also give a more detailed insight into the effect of applying S2 to estimate the surface water area.

Next, the winter months for the reservoirs are causing an increased number of noisy images. Hence in the future, a potential machine learning algorithm could be developed to determine these images by order of weights. For instance, the NDSI could estimate the reservoirs' water extent in months where snow is significantly more present. Furthermore, removing the noise prior to the analysis could enhance the water-level time series and, therefore, the potential to monitor the volume.

The L&R considered for this thesis was only located in the USA. Therefore, the global implementation of both LBDEM and the ability to monitor the volume time series should be further researched. For example, consider alternative in-situ data from countries like Spain, South Africa, and India while comparing other elevation models.

Future research should consider an updated selection algorithm for determining the optimal DEM based on the number of flat elevations. Thus, providing an insight if ALOS would still be the optimal choice when the extrapolated depths of LBDEM replace the flat pixels.

Regarding the extraction of the water level, an improvement can be made regarding the border between water and land. As of now, the border pixels take the DEM pixels that have the most overlap. However, hypothetically due to the large pixel size of SRTM or ALOS, it could still introduce an error in the elevation distribution. Therefore, an analysis should be made on how to determine the elevation found in the border pixels.

Please note that this study did not consider the filling operation, demonstrated by e.g., Donchyts (2018) study or the estimation of the water/land border by use of radar images (i.e., S1). These images can be a helpful alternative/addition to the temporal cloud smoothing filter, reducing the water level error.

Likewise, while using this filling operation, an insight can be given to what extent the reservoir's surface should be seen since the boundary of the reservoir could be distinguished from the clouds at only the usable area. Therefore, only a filling or cloud smoothing filter is needed to apply for the images where the L&R was not correctly located

Lastly, the volume levels are indirectly affected by the surface water extent constructed by the multispectral imagery data. Therefore, a validation procedure can be developed that would give an insight into the method's accuracy in regions where in-situ data is not available. Since the surface area extent can be computed using the water level input relative to the choice DEM. With the inundated region, the surface area could be re-computed and compared to the results of, i.e., S2. When a significant difference is experienced between these two at a given moment in time, the volume level could be considered inaccurate, validating the method's effectiveness at objects with little in-situ data.

Appendix-A: Selected equations

Otsu thresholding

So, to find this threshold that finds the minimum between the classes' variance, the following equation is applied:

$$t = argmin(\sigma_w(t))^2 \quad \text{(A1)}$$

Here σ is the variance that is within the classes. This is defined by:

$$\sigma_w^2(t) = w_0^2(t) \cdot \sigma_0^2(t) + w_1^2(t) \cdot \sigma_1^2(t) \quad \text{(A2)}$$

Where w and sigma are the representing the variances and probabilities of the classes (i.e., Land and Water). The separation index t is threshold value. This *t* can be found by creating a histogram of L levels, where the probability is defined as $W_{0,1}$ by

$$w_o(t) = \sum_{\{i=0\}}^{t} p(i) \quad \text{(A3)}$$
$$w_1(t) = \sum_{\{i=t+1\}}^{\{L-1\}} p(i) \quad \text{(A4)}$$

When minimizing the sum of A3 and A4 for each possible threshold can become tentative. Hence Otsu gives a solution that the same result can be achieved for minimizing the different class variance (instead of determining the maximizing). This step is formulated as follows:

$$\sigma_b^2 = \sigma^2 - \sigma_w^2(t) = w_0(\mu_0(t) - \mu)^2 + w_1(\mu(t) - \mu)^2 \quad \text{(A5)}$$
$$\sigma_b^2(t) = w_0(t) \cdot w_1(t)(\mu_0(t) - \mu_1(t)) \quad \text{(A6)}$$

Hence the optimal threshold that can be achieved is by applying the following equation:

$$t = argmax(\sigma_b^2(t)) \quad \text{(A7)}$$

Canny edge detection

The gradient is computed according the following equation value from the (such as Prewitt equation) returns a derivative in both directions (x,y):

$$G = \sqrt{\{G_x^2 + G_y^2\}} \quad \text{(A8)}$$

$$\Phi = atan2(G_y, G_x) \quad \text{(A9)}$$

Hence G is the gradient that results from both directions, whilst the Φ of A9 gives the direction of the gradient. When a gradient having a smaller magnitude are suppressed for finding the highest gradient between land and water.

Appendix-B: Additional information volume selected L&R

Consider that the Optimal DEM was selected based on the volume correlation coefficient.
*Here the in-situ data had a shift in the time series, caused by effects not known to the author.

Name	Max. Surface Area [km2]	Range In-situ WL [m]	DEM optimal	Region [%] no flatting	R^2 - WL	R^2 -VOL	RMSE [km^3]
Monroe City	0.3	2	ALOS	44	0.10	0.06	7.0 e-5
Concordia	0.9	2	ALOS	64	0.16	0.08	0.1 e-3
Trinidad	2.7	11	ALOS	84	0.96	0.94	2.2 e-3
Maloya	0.4	2	NED	22	0.70	0.26	2.7 e-3
Greenbelt	2.7	4	ALOS	54	0.87	0.85	1.2 e-2
Vail	1.6	6	SRTM	29	0.56	0.56	3.0 e-3
Piru.	2.4	24	NED	42	0.92	0.94	1.4 e-2
Eleanor	3.8	15	SRTM	8.9	0.57	0.60	1.6 e-2
Donnel*	1.6	-	SRTM	33	0.12	0.12	4.7 e-2
Beardsley	2.7	37	NED	2.3	0.56	0.81	6.1 e-3
Tulloch	3.5	10	SRTM	27	0.49	0.17	4.9 e-3
Wynoochee	2.9	19	ALOS	88	0.60	0.60	4.9 e-2
Howard A Hanson	1.8	30	ALOS	84	0.56	0.69	1.6 e-2
Teller*	0.6	-	ALOS	87	0.2	0.33	1.2 e-3
Nambe Falls	0.2	9	SRTM	50	0.83	0.78	6.41
Mcclure	0.2	17	SRTM	24	0.86	0.91	4.8 e-4
Nichols	0.09	10	SRTM	99	0.71	0.73	1.5 e-5
Rifle Gap	1.0	13	NED	31	0.88	0.88	5.5 e-4
Vega.	2.3	16	SRTM	25	0.89	0.89	5.8 e-3
Silver Jack	1.0	23	ALOS	83	0.50	0.51	3.8 e-3
Crawford	0.9	21	NED	3	0.91	0.95	5.9 e-3
Paonia	1.0	27	SRTM	51	0.78	0.84	4.8 e-3
Fruit Growers	1.0	8.6	ALOS	82	0.34	0.64	1.2 e-3
Ridgway	3.2	13	SRTM	14	0.87	0.87	3.1 e-2
Lemon	1.8	26	ALOS	65	0.76	0.70	9.5 e-3
Prosser Creek	1.7	16	ALOS	70	0.84	0.84	3.8 e-3
Boca	2.6	18	ALOS	94	0.80	0.84	1.9 e-2
El Capitain	2.8	11	SRTM	21	0.92	0.92	2.6 e-2
Santa Ynez	0.7	11	NED	26	0.82	0.83	2.2 e-3
Alisal	0.3	7	ALOS	64	0.87	0.86	1.3 e-3

Table 8 Additional information of the volume variability selected L&R

References

Arrish, C. E.-S. (2019). Validation of ICESat-2 ATLAS bathymetry and analysis of ATLAS's bathymetric mapping performance. *Remote Sensing, 11*(14), 1634.

Abileah, R. a. (2011). A completely remote sensing approach to monitoring reservoirs water volume. *Int. Water Technol. J*, 63--77.

Amitrano, D. a. (2014). Sentinel-1 for monitoring reservoirs: A performance analysis. *Remote Sensing*, 10676--10693.

Avisse, N. T. (2017). Monitoring small reservoirs' storage with satellite remote sensing in inaccessible areas. *Hydrology and Earth System Sciences, 21*(12), 6445-6459.

AHN. (2020, Mar). *Distributie*. From Actueel Hoogtebestand Nederland: https://www.ahn.nl/distributie

ALOS-Project. (n.d.). *ALOS-2 Project / PALSAR-2*. From ALOS-Project: https://www.eorc.jaxa.jp/ALOS-2/en/about/palsar2

Ballatore, T. V. (n.d.). The case for a world lake vision. *Hydrological processes*(16), 2079-2089.

Bonnema, M. a. (2017). Inferring reservoir operating patterns across the Mekong Basin using only space observations. *Water Resources Research*, 3791--3810.

Canny, J. (1986). A computational approach to edge detection. *IEEE Transactions on pattern analysis and machine intelligence*, 679--698.

Chawla, I. a. (2020). A review of remote sensing applications for water security: Quantity, quality, and extremes. *Journal of Hydrology, 585*, 124826.

Cohen, S., A. R.-F.-P. (2019). The Floodwater Depth Estimation Tool (FwDET v2.0) for improved remote sensing analysis of coastal flooding. *Natural Hazards Earth Systems Sciences*, 2053–2065.

Collins, J. a. (2015). Applying terrain and hydrological editing to TanDEM-x data to create a consumer-ready worldDEM product. *International Archives of the Photogrammetry, Remote Sensing \& Spatial Information Sciences*.

Crétaux, J.-F. a.-N. (2015). Global surveys of reservoirs and lakes from satellites and regional application to the Syrdarya river basin. *Environmental Research Letters, 10*(1), 015002.

Crippen, R. a. (2016). *NASADEM global elevation model: Methods and progress.* Pasadena, CA: Jet Propulsion Laboratory, National Aeronautics and Space.

Deng, X. a. (2020). Remote sensing estimation of catchment-scale reservoir water impoundment in the upper Yellow River and implications for river discharge alteration. *Journal of Hydrology*, 124791.

Diekkrüger, &. L. (2002). *Estimation of water storage capacity and evaporation losses of small reservoirs in the upper east region of Ghana.* Bonn: Universität Bonn.

Di Baldassarre, G. a. (2018). Water shortages worsened by reservoir effects. *Nature Sustainability*, 617--622.

Donchyts, G. a. (2016). A 30 m resolution surface water mask including estimation of positional and thematic differences using landsat 8, srtm and openstreetmap: a case study in the Murray-Darling Basin, Australia. *Remote Sensing*, 386.

Donchyts, G. (2018). *Planetary-scale surface water detection from space.* Delft: Technische Universiteit Delft.

Eilander, D. M. (2013). *Remotely sensed small reservoir monitoring: A Bayesian approach.* Delft: Delft University of Technology.

Fernandez, A. a. (2016). Analysis of the behavior of three digital elevation model correction methods on critical natural scenario. *Journal of Hydrology: Regional Studies*, 304--315.

Fouladinejad, F. a. (2019). HISTORY AND APPLICATIONS OF SPACE-BORNE LIDARS. *International Archives of the Photogrammetry, Remote Sensing & Spatial Information Sciences*.

Frappart, F. a.-L. (2018). Influence of recent climatic events on the surface water storage of the Tonle Sap Lake. *Science of the Total Environment*, 1520--1533.

Gesh, D. O. (68). The National elevation dataset. *Photogrammetric engineering and remote sensing*, 5-32.

Hang, S. a. (2016). Bathymetric survey of water reservoirs in north-eastern Brazil based on TanDEM-X satellite data. *Science of the Total Environment*, 575--593.

Hayes, N. M. (2017). Key differences between lakes and reservoirs modify climate signals: A case for a new conceptual model. *Limnology and Oceanography Letters, 2*(2), 47--62.

Huang, C. a. (2018). Detecting, extracting, and monitoring surface water from space using optical sensors: A review. *Reviews of Geophysics*, 333--360.

Ji, L. a. (2009). Analysis of dynamic thresholds for the normalized difference water index. *Photogrammetric Engineering & Remote Sensing*, 1307--1317.

Lehner, B. a. (2011). High-resolution mapping of the world's reservoirs and dams for sustainable river-flow management. *Frontiers in Ecology and the Environment*, 494--502.

Liebe, J. a. (2005). Estimation of small reservoir storage capacities in a semi-arid environment: A case study in the Upper East Region of Ghana. *Physics and Chemistry of the Earth, Parts A/B/C, 30*, 448--454.

Ma, Y. a. (2020). Satellite-derived bathymetry using the ICESat-2 lidar and Sentinel-2 imagery datasets. *Remote Sensing of Environment*, 112047.

McFeeters, S. K. (1996). The use of the Normalized Difference Water Index (NDWI) in the delineation of open water features. *International journal of remote sensing, 17*(7), 1425--1432.

NASA. (2018, Oct). *National Snow and Ice Data Center*. From ICESat-2 Data Sets at NSIDC | National Snow and Ice Data Center: https://nsidc.org/data/icesat-2/data-sets

Neumann, T. A. (2019). The Ice, Cloud, and Land Elevation Satellite--2 Mission: A global geolocated photon product derived from the advanced topographic laser altimeter system. *Remote sensing of environment*, 111325.

Neuenschwander, A. L. (2016). The potential impact of vertical sampling uncertainty on ICESat-2/ATLAS terrain and canopy height retrievals for multiple ecosystems. *Remote Sensing*, 10--39.

Nikolakopoulos, K. G. (2020). Accuracy assessment of ALOS AW3D30 DSM and comparison to ALOS PRISM DSM created with classical photogrammetric techniques. *European Journal of Remote Sensing*, 39--52.

Nisha, R. M. (2015). Reservoir Storage Measurement & Recordkeeping Guide for above ground reservoirs. *International Journal of Engineering Trends and Technology (IJETT)*, 48--53.

Otsu, N. (1979). A threshold selection method from gray-level histograms. *IEEE transactions on systems, man, and cybernetics, 9*(1), 62--66.

Pan, F. a. (2019). A MATLAB-based digital elevation model (DEM) data processing toolbox (MDEM). *nvironmental Modelling & Software*, 104566.

Parrish, C. E.-S. (2019). Validation of ICESat-2 ATLAS bathymetry and analysis of ATLAS's bathymetric mapping performance. *Remote Sensing*, 1634.

Pekel, J.-F. a. (2016). High-resolution mapping of global surface water and its long-term changes. *Nature*, 418--422.

Peng, D. a. (2006). Reservoir storage curve estimation based on remote sensing data. *Journal of Hydrologic Engineering*, 165--172.

Pham-Duc, B. a. (2017). Surface water monitoring within Cambodia and the Vietnamese Mekong Delta over a year, with Sentinel-1 SAR observations. *Water*, 366.

Pipitone, C. a. (2018). Monitoring water surface and level of a reservoir using different remote sensing approaches and comparison with dam displacements evaluated via GNSS. *Remote Sensing*, 71.

Sanborn. (2018, October). *Hydro Flattening*. From Total Geospatial Solutions: https://www.sanborn.com/hydro-flattening/

Santillan, J. a.-S. (2016). Vertical Accuracy Assessment of 30-M Resolution Alos, Aster, and Srtm Global Dems Over Northeastern Mindanao, Philippines. *International Archives of the Photogrammetry, Remote Sensing & Spatial Information Sciences}, 41*.

Sauer, V. B. (2010). Techniques and Methods. In V. B. Sauer, *Stage measurement at gaging stations.* Reston, VA: U.S. Geological Survey.

Stéphane, M. &. (2009). Digital elevation model computation with Spot-5 panchromatic and mutispectral images using low stereoscopic angle and geomteric model refinement. *IEEE International Geosciences and Remote Sensing Symposium*, IV-442.

Tadono, T. a. (2014). Precise global DEM generation by ALOS PRISM. *ISPRS Annals of the Photogrammetry, Remote Sensing and Spatial Information Sciences*, 71.

Takaku, J. a. (2020). Updates of 'AW3D30'ALOS Global Digital Surface Model with Other Open Access Datasets. *The International Archives of Photogrammetry, Remote Sensing and Spatial Information Sciences*, 183--189.

Tarpanelli, A. a. (2019). On the potential of altimetry and optical sensors for monitoring and forecasting river discharge and extreme flood events. In A. a. Tarpanelli, *Extreme Hydroclimatic Events and Multivariate Hazards in a Changing Environment* (pp. 267--287). Elsevier.

U.S. Department of the Interior. (2019, August 1). *Storage Capacity of Lake Mead*. From NationalParkService: https://www.nps.gov/lake/learn/nature/storage-capacity-of-lake-mead.htm

Uuemaa, E. a. (2020). Vertical accuracy of freely available global digital elevation models (ASTER, AW3D30, MERIT, TanDEM-X, SRTM, and NASADEM). *Remote Sensing*, 3482.

Vanthof, V. a. (2019). Water storage estimation in ungauged small reservoirs with the TanDEM-X DEM and multi-source satellite observations. *Remote Sensing of Environment*, 111-437.

Venot, J.-P. a. (2012). Revisiting dominant notions: a review of costs, performance and institutions of small reservoirs in sub-Saharan Africa. *IWMI*.

Weekley, D. a. (2021). Tracking Lake Surface Elevations with Proportional Hypsometric Relationships, Landsat Imagery, and Multiple DEMs. *Water Resources Research*, Wiley Online Library.

Wisser, D. a. (2013). Beyond peak reservoir storage? A global estimate of declining water storage capacity in large reservoirs. *Water Resources Research, 49*(9), 5732--5739.

Xu, N. a. (2020). Monitoring Annual Changes of Lake Water Levels and Volumes over 1984--2018 Using Landsat Imagery and ICESat-2 Data. *Remote Sensing, 12*(23), 4004.

Xu, H. (2006). Modification of normalised difference water index (NDWI) to enhance open water features in remotely sensed imagery. *International journal of remote sensing, 27*(14), 3025--3033.

Zhang, S. a. (2014). Monitoring reservoir storage in South Asia from multisatellite remote sensing}. *Water Resources Research*, 8927--8943.